ELSEVIER

J. Non-Newtonian Fluid Mech. 117 (2004) 25–46

Journal of Non-Newtonian Fluid Mechanics

www.elsevier.com/locate/jnnfm

Turbulent flow of viscoelastic liquids through an axisymmetric sudden expansion

R.J. Poole*, M.P. Escudier

Department of Engineering, Mechanical Engineering, University of Liverpool, Brownlow Hill, Liverpool L69 3GH, UK

Received 11 August 2003; received in revised form 23 September 2003; accepted 24 November 2003

Abstract

An experimental investigation is reported of turbulent flow of three concentrations (0.02, 0.05 and 0.1 wt.%) of an aqueous solution of a polyacrylamide (PAA) through an axisymmetric sudden expansion of area-expansion ratio 4. PAA is a viscoelastic, shear-thinning liquid and two water flows are reported for comparative purposes. For water and the two lowest PAA concentrations, the flow was axisymmetric and large increases in the reattachment length (approximately double the water values) found for these PAA flows. At the highest concentration, 0.1% PAA, the flow was strongly asymmetric and the reattachment length up to three times the value for water.

Keywords: Viscoelastic; Shear thinning; Turbulent; Axisymmetric sudden expansion

1. Introduction

The turbulent flow of fluids through sudden expansions has both fundamental scientific interest and numerous practical applications: such flows occur, for example, in pipe-flow systems in the chemical, pharmaceutical and petroleum industries, in air-conditioning ducts, in dump combusters and in fluidic devices. So far as Newtonian fluids are concerned, much of the fundamental understanding of turbulent free shear layers and separated internal flows has resulted from investigations of the flow through a sudden expansion or over a backward-facing step. Indeed the developers of turbulence codes relied heavily on experimental data for these flows, and in particular the backward-facing step geometry, to validate and improve their simulations.

Although many naturally occurring fluids, and the majority of synthetic fluids, such as those encountered in the food, processing and chemical industries, are non-Newtonian in character, the existing literature is almost devoid of both experimental and computational studies of the turbulent flow of non-Newtonian fluids in any situation other than fully-developed pipe or duct flow. Most research into the turbulent flow of non-Newtonian liquids has been concerned with the important, but still not completely understood, phenomenon of drag reduction in pipe or duct flow. In recent experimental studies the present authors (Poole and Escudier [1–3]) have investigated the turbulent flow of a series of non-Newtonian liquids through two plane sudden expansions. We have reported ([1,2]) results for an expansion ratio ($R = D/d$) of 1.43, which acts essentially as a double backward-facing step, and also [3] for the turbulent flow of a strongly viscoelastic liquid through a plane sudden expansion of modest aspect ratio (5.33) and an expansion ratio of 4. The study reported here extends this work by examining the turbulent flow of a series of strongly viscoelastic liquids through an axisymmetric sudden expansion with an area expansion ratio of 4.

Despite the fact that the axisymmetric sudden expansion is arguably a more practically relevant configuration than the backward-facing step, the available literature for Newtonian fluid flows is far less extensive [1,2]. There are a number of differences compared to backward-facing step flow. The reattachment length for the latter is 8–11 step heights compared to 5–8 step heights. Devenport and Sutton [4] attribute this difference to the fact that, relative to the surface area available for entrainment, the separated shear layer has to entrain a greater volume of recirculating fluid before reattaching in the axisymmetric geometry compared with the two-dimensional case. Variations in the reattachment length between studies are, as is the case for backward-facing step flow, primarily a consequence

* Corresponding author.
E-mail address: robpoole@liv.ac.uk (R.J. Poole).

0377-0257/$ – see front matter © 2003 Elsevier B.V. All rights reserved.
doi:10.1016/j.jnnfm.2003.11.007

Nomenclature

a	constant in Carreau–Yasuda model
b	constant in power-law formula for N_1
c	concentration by weight of PAA (%)
C_P	pressure coefficient ($= \Delta p/0.5\rho U_B^2$)
d	pipe diameter at inlet (m)
D	downstream pipe diameter (m)
D_{PIPE}	pipe diameter upstream of smooth contraction (m)
De	Deborah number (λ/T)
h	step height (m)
k	turbulent kinetic energy (m/s)
m	power-law index in power-law formula for N_1
n	power-law index in Carreau–Yasuda model
N_1	first normal-stress difference (Pa)
p	wall-pressure (Pa)
$\dot{Q}_A$	apparent flowrate determined by numerical integration (m^3/s)
$\dot{Q}_F$	flowrate determined from flowmeter (m^3/s)
$\dot{Q}_R$	apparent recirculating flowrate determined by numerical integration (m^3/s)
r	radial distance from centreline (m)
R_{PIPE}	pipe radius downstream of expansion (m)
R	area expansion ratio ($= (D/d)^2$)
Re	Reynolds number ($= \rho h U_B/\mu_{SEP}$)
Re_{CH}	Reynolds number ($= \rho h U_B/\mu_{CH}$)
T	characteristic time of fluid deformation process (s)
u'	axial rms turbulence intensity (m/s)
u'_{MAX}	maximum axial rms turbulence intensity (m/s)
u'_{SEP}	maximum axial rms turbulence intensity at $x/h = 1$ (m/s)
U	mean axial velocity (m/s)
U_B	bulk mean velocity ($4\dot{Q}_F/(\pi d^2)$)(m/s)
U_E	centreline velocity (m/s)
U_{RMAX}	maximum recirculating streamwise/axial velocity (m/s)
$\overline{uv}$	Reynolds shear stress (m^2/s^2)
v'	radial rms turbulence intensity (m/s)
v'_{MAX}	maximum radial rms turbulence intensity (m/s)
v'_{SEP}	maximum radial rms turbulence intensity at $x/h = 1$ (m/s)
w'	tangential rms turbulence intensity (m/s)
w'_{MAX}	maximum tangential rms turbulence intensity (m/s)
w'_{SEP}	maximum tangential rms turbulence intensity at $x/h = 1$ (m/s)
x	axial distance from expansion (m)
x_R	reattachment length (m)
X_R	non-dimensional reattachment length (x_R/h)
y	radial distance from wall (m)

Greek letters

β	diameter ratio d/D (0.5)
δ_ω	vorticity thickness ($U_E/\dot{\gamma}_{MAX}$) (m)
$\dot{\gamma}$	shear rate (s^{-1})
λ	relaxation (or characteristic) time of fluid (s)
λ_{CY}	time constant in Carreau–Yasuda model (s)
μ	shear viscosity ($= \tau/\dot{\gamma}$) (Pa s)
μ_{CH}	Carreau–Yasuda viscosity corresponding to characteristic shear-rate ($\dot{\gamma} = U_B/h$) (Pa s)
μ_{CY}	viscosity corresponding to Carreau–Yasuda model (Pa s)
μ_M	measured shear viscosity (Pa s)
ψ_R	stream function between wall and centreline ($2\pi\int_0^R ur\,dr$)
μ_0	zero-shear-rate viscosity (Pa s)
μ_∞	infinite-shear-rate viscosity (Pa s)
μ_{SEP}	Carreau–Yasuda viscosity corresponding to shear-rate at $x/h = 1$ (Pa s)
ρ	density (kg/m^3)
τ	shear stress (Pa)
ψ	stream function ($= 2\pi\int_0^r ur\,dr$)

of different inlet conditions. So drew the conclusion that 'the single most important parameter that affects the reattachment length is the inlet centreline turbulence intensity or some other parameter that tends to promote growth in the separating shear layer' [5]. That 'other parameter' may be, as was the case with backward-facing steps [1,2], the maximum turbulence intensity at separation, although the available data in the literature is less conclusive in the axisymmetric case than it is for flow over a backward-facing step. For example, the large differences in reattachment length x_R for the very similar inlet turbulence intensity and expansion ratio of Gould et al. ($x_R = 8$ step heights) [6] and Pereira and Pinho ($x_R = 10$ step heights) [7], may be due to different boundary-layer thicknesses. The maximum turbulence intensities for all the results reported in the literature show that $u' > w' > v'$. Kasagi and Matsunga [8], the only authors to measure all three turbulence intensities *reliably* for a backward-facing step, also observed this ordering.

In contrast to the complete lack of planar sudden-expansion data prior to our recent work [1–3], limited progress has been made in understanding turbulent recirculating and reattaching non-Newtonian fluid flow in the axisymmetric sudden-expansion configuration. Castro and Pinho [9], Pereira and Pinho [7,10,11] have investigated the flow of a series of non-Newtonian liquids with fully-developed inlet velocity profiles through an axisymmetric sudden expansion of expansion ratio 1.54 (of more relevance in [7] is their work with an identical area expansion ratio ($R = 4$) to the present study, albeit with different polymer solutions). Castro and Pinho [9] used Tylose solutions (0.4 and 0.5%), which are moderately shear thinning (power law index ≈0.7) and practically inelastic. They noted only small changes in

the mean flow but reductions up to 30% of the Reynolds normal stresses, u', v' and w'. Pereira and Pinho [10] used 0.2% xanthan gum as their working fluid, as did Escudier and Smith [12] in a companion study of identical expansion ratio but with a smooth contraction preceding the expansion which produced a uniform inlet profile with low freestream turbulence intensity. Escudier and Smith [12] observed no significant change in the mean flow but turbulent kinetic energy levels reduced by up to 20%. In contrast Pereira and Pinho [10] reported a reduction in the reattachment length of more than 20% relative to a Newtonian fluid flow with a similar Reynolds number. This difference was attributed to the dominating role of inlet turbulence with higher axial turbulence intensity and lower levels of turbulence anisotropy at inlet associated with their fully-developed inlet flow. Isomoto and Honami [13] observed the same influence for Newtonian fluid flow over a backward-facing step. Pereira and Pinho [11] concluded that both for the mean flow and the turbulent structure the flow of a 1% Laponite solution, a shear-thinning, thixotropic, essentially inelastic fluid, was little different to that of water.

Pak et al. [14] used flow visualisation to investigate the flow of two non-Newtonian liquids through an axisymmetric sudden expansion (as in the current study the expansion was preceded immediately by a smooth contraction): a purely viscous shear-thinning liquid, Carbopol (concentrations 0.5, 1.0 and 1.5%), and viscoelastic polyacrylamide solutions (0.02, 0.05 and 0.1%). The reattachment lengths for Carbopol were found to be essentially the same as for water whereas for the polyacrylamide solutions they were two to three times longer than those for water, increasing with the concentration. They hypothesised that this increase was a consequence of suppressed eddy motions within the shear layer resulting from viscoelastic effects.

The objective of the current study is to examine the influence shear thinning and viscoelasticity have on the turbulent reattachment process downstream of an axisymmetric sudden expansion. The three concentrations of polyacrylamide solutions, chosen to match those used by Pak et al. [14], encompass a wide range of non-Newtonian characteristics: a dilute solution, 0.02%, which in pipe flow produces high levels of drag reduction but is only slightly shear-thinning and exhibits low measurable elasticity; an intermediate concentration, 0.05%, which is both moderately shear-thinning and elastic and a relatively high concentration, 0.1%, which is both highly shear-thinning and elastic.

2. Experimental rig and instrumentation

Apart from a different expansion module, the flow loop used for the present experiments was identical to that used by Escudier and Smith [12] in their investigation of flow through an axisymmetric sudden expansion. The expansion used here was located 9.5 m from the inlet of the test section and was preceded by a short (135 mm in length), smooth contraction (150 mm concave radius followed by 75 mm convex radius). The pipe diameter upstream of the contraction was $D_{\mathrm{PIPE}} = 100.4$ mm, the pipe diameter at the inlet to the expansion was $d = 26$ mm, the step height was $h = 13$ mm and the downstream pipe diameter therefore $D = 52$ mm. These dimensions produce an expansion ratio $R = D/d = 2$ and an area expansion ratio $(D/d)^2 = 4$. The main body of the sudden expansion, the key dimensions of which are shown in Fig. 1, was made of perspex. The smooth contraction was fabricated from stainless steel which restricted optical access at the inlet plane so that no axial velocities could be measured at $x/h = 0$. Distributions of mean velocity and turbulence structure were obtained from traverses at 12 axial locations corresponding to x/h values of 1, 2, 3, 4, 5, 6, 8, 9, 10, 12, 16 and 20. Due to the higher shear rates present in axisymmetric sudden expansion flows, degradation of the PAA solutions occurs much more quickly than for flows through plane expansions [1,2,3], with low concentrations being especially susceptible. Data is not presented for $x/h = 2$ and 10 for 0.02 and 0.05% PAA. For the 0.02% concentration degradation occurred after about 8–10 h of flow at ~11 m^3/h (a mid-range flowrate for our pump), with this time decreasing with increasing flowrate. Fluid degradation was monitored both by checking the fluid viscosity

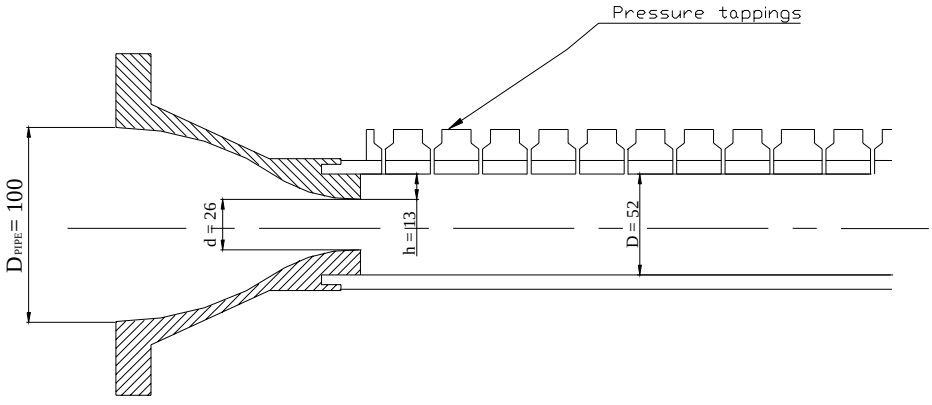

Fig. 1. Axisymmetric sudden expansion geometry and inlet contraction, dimensions in mm.

and also by observing the turbulence statistics to see if they were internally consistent with previously obtained data as increases in v' and w' were observed as the fluid degraded. The most sensitive indicator of fluid degradation was the maximum tangential turbulence intensity at inlet. When this had altered by more than 10% the fluid was judged to have degraded and to achieve consistent results the fluid then had to be dumped and a fresh batch mixed. This was usually necessary after only 5–6 profiles: the results presented here for both 0.02 and 0.05% PAA were obtained from five different fluid batches over a 10-week period for each concentration.

The Dantec Fibreflow laser Doppler anemometer (LDA) system used for the velocity and turbulence measurements comprised a Dantec 60X10 probe and a Dantec 55X12 beam expander in conjunction with two Dantec Burst Spectrum Analyzer signal processors (one model 57N10, the other model 57N20). The beam separation at the front lens was 51.5 mm and the lens focal length 160 mm (corresponding to an included half angle of 9.14°) which produces a measurement volume with principal axis of length 0.21 mm and diameter 20 μm. In view of the small diameter of the measuring volume, no correction was applied for the effect of velocity-gradient broadening. As recommended by Tropea [15], transit-time weighting was used to correct the velocity measurements for the effects of velocity bias. For the axial and tangential components, measurements were taken along a horizontal radial line starting at the side of the expansion closest to the LDA optics. For the radial component, measurements were taken along a vertical radial line passing through the centreline of the expansion. At each location, nominally 10,000 velocity samples were collected which resulted in a maximum relative statistical error, for a 95% confidence interval, of approximately 0.5% in the mean velocity and 1.4% in the turbulence intensity (Yanta and Smith [16]). The total uncertainty in the mean velocity is estimated to be in the range 3–4% and in the range 6–7% for the turbulence intensities.

As shown in Fig. 1, 19 pressure tappings of 1 mm diameter were provided along the top of the expansion to allow the wall-pressure distribution to be measured. The tappings were connected to 2 mm i.d. clear vinyl tubing, filled with deionised water, which linked each in turn via a series of valves to a Validyne differential pressure transducer (model DP15-26). Flow rates were measured using a Fischer and Porter electromagnetic flowmeter (model 10D1) incorporated in the flow loop upstream of the sudden expansion with the flowmeter output signal recorded via an Amplicon PS 30AT A/D converter.

All rheological measurements were carried out using a TA Instruments Rheolyst AR 1000N controlled-stress rheometer. A temperature of 20 °C was maintained for the rheological measurements, which was also the average temperature of the fluid for the duration of the experimental runs. Control of the temperature of the sample to within ±0.1 °C is achieved in the rheometer via a plate using the Peltier effect.

3. Rheology of working fluids

The working fluids used in this investigation were various concentrations of aqueous solutions of a polyacrylamide (PAA), Separan AP273 E supplied by SNF UK limited. The solvent used was filtered tap water with 100 ppm of 40% formaldehyde solution (i.e. 4×10^{-3}% concentration) added to retard bacterial degradation. Approximately 0.25 g of Timiron seeding particles (average size 5 μm) were added to the fluid (total volume of fluid 575 l) to improve the LDA signal quality.

PAA was chosen as the working fluid as it is highly viscoelastic, is optically transparent (thereby permitting LDA measurements) and has been used extensively in previous investigations in our laboratory (Escudier et al. [2,12,17]) and elsewhere (e.g. den Toonder et al. [18] and Stokes et al. [19]). According to Walters et al. [20] PAA is very flexible in its molecular structure and this gives rise to its increased elastic properties compared to other water-soluble polymers, such as xanthan gum and carboxymethylcellulose. The average molecular weight for the PAA used in this study, ascertained using gel-phase chromatography, was determined to be 1.94×10^6 kg/kmol with a polydispersity of 1.05. The flow curve (i.e. viscosity versus shear rate) for PAA is shown in Fig. 2 together with the corresponding Carreau–Yasuda model fit:

$$\mu_{CY} = \mu_\infty + \frac{\mu_0 - \mu_\infty}{(1 + (\lambda_{CY}\dot{\gamma})^a)^{n/a}}$$

where μ_0 is the zero-shear-rate viscosity, μ_∞ the infinite-shear-rate viscosity, λ_{CY} a time constant, n a power-law index and a a parameter introduced by Yasuda et al. [21]. The model parameters, which are listed in Table 1, were determined using the fitting procedure outlined in Escudier et al. [22], in essence minimisation of the standard deviation, $(1 - \mu_M/\mu_{CY})^2$. The measured variation of the first normal stress difference N_1, which is a good indicator of the level of elasticity of a fluid, versus shear stress τ is shown for the highest concentration of PAA (i.e. 0.1%) in Fig. 3. For the lower concentrations (0.02 and 0.05%) the N_1 values produced were below the sensitivity of the rheometer even at the highest shear stresses. It should be noted that at the lowest shear stress that we could measure ($\tau = 0.01$ Pa) a highly elastic liquid (i.e. the recoverable shear $N_1/2\tau > 0.5$, Barnes et al. [23]) would only produce an N_1 value of the order of 10 mN which is within the effective resolution of our instrument confirming that the fluid could be regarded as essentially inelastic. A power-law fit to the N_1 (τ) data

Table 1
Carreau–Yasuda model parameters

c (%)	μ_0 (Pa s)	μ_∞ (Pa s)	λ_{CY} (s)	n	a
0.02	0.0220	0.00262	0.551	0.623	0.623
0.05	0.614	0.00282	25.7	0.578	0.989
0.1	8.83	0.00437	104	0.679	0.969

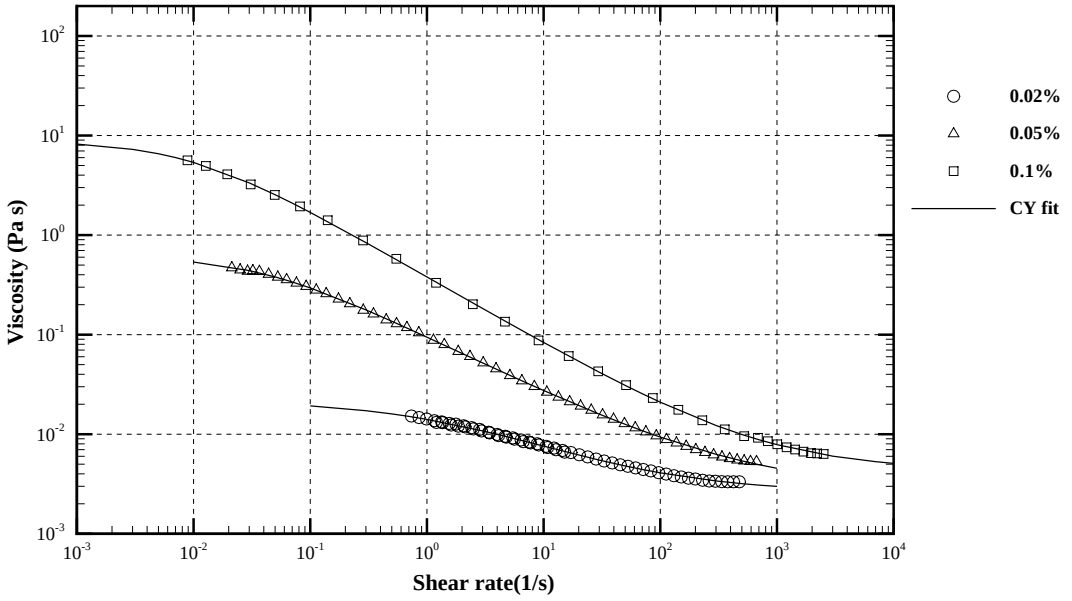

Fig. 2. Viscosity vs. shear rate for 0.02, 0.05 and 0.1% polyacrylamide (including Carreau–Yasuda fit).

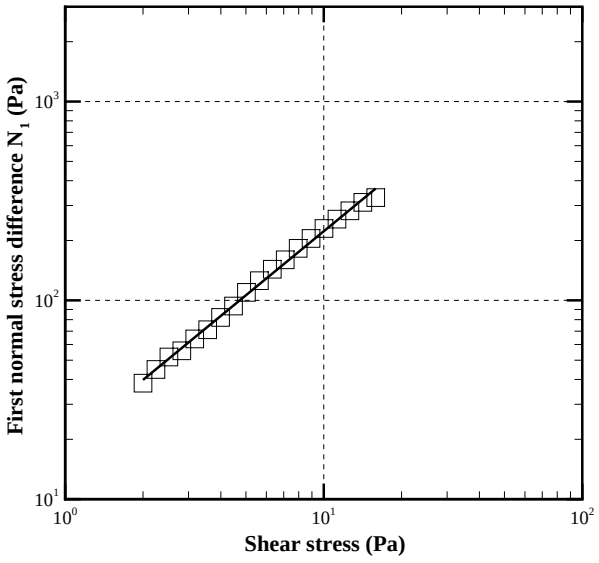

Fig. 3. First normal-stress difference vs. shear stress for 0.1% polyacrylamide.

has been included in Fig. 3 and the parameters are listed in Table 2. In the measured range for 0.1% PAA, the recoverable shear $N_1/2\tau$ is much >0.5 indicating a highly elastic liquid.

Table 2
Power-law parameters for normal-stress variation ($N_1 = b\tau^m$)

Fluid (%)	0.1
Range of τ (Pa)	2.0–16
b (Pa^{1-m})	19.0
m	1.07

4. Turbulent flow of viscoelastic liquids

4.1. Mean flow

In the interest of clarity the experimental results have been separated into four sets: (A) Newtonian, (B) 0.02% PAA, (C) 0.05% PAA and (D) 0.1% PAA. To define a Reynolds number we have used the bulk velocity U_B at inlet to the expansion determined from the flowrate as the velocity scale and the step height $h = 13$ mm as the length scale. The density of all the solutions was practically that of the solvent, water. To obtain a viscosity for the viscoelastic liquids we have estimated the maximum shear rate from the velocity distribution at the first measurement plane ($x/h = 1$) and then substituted this value into the Carreau–Yasuda model. This approach differs slightly from the methodology adopted in our previous work [1–3] where the shear rate at separation (i.e. $x/h = 0$) was used. Lack of optical access through the stainless steel contraction that precedes the expansion (explained in Section 2), precluded measurements at the inlet thereby necessitating this difference in approach. However it is worth noting that the shear rate at separation will always be greater than the maximum shear rate at $x/h = 1$, the characteristic viscosity will therefore be lower, and hence the Reynolds number higher. It is also possible to obtain a Reynolds number based on a characteristic viscosity, such as the viscosity corresponding to $\dot{\gamma} = U_B/h$. It is easily seen that this Re_{CH} will always be lower than the choice we have adopted and is included in Table 3 for comparative purposes. In the discussion which follows, when not explicitly stated, all reference to mean-flow parameters and turbulence quantities are to the non-dimensional values. For each non-Newtonian fluid flow data set the Newtonian fluid flow

Table 3
Representative mean flow and turbulence characteristics for an axisymmetric sudden expansion with $h = 13$ mm, $D = 52$ mm.

Fluid	Re ($\equiv \rho U_b h/\mu_{SEP}$)	Re_{CH} ($\equiv \rho U_b h/\mu_{CH}$)	u'_0/U_B	u'_{SEP}/U_B	v'_{SEP}/U_B	w'_{SEP}/U_B	U_{RMAX}/U_B	u'_{MAX}/U_B	v'_{MAX}/U_B	w'_{MAX}/U_B	$(\dot{Q}_R/\dot{Q}_A)$ (%)	X_R (x_R/h)
Water	30000	30000	<0.02	0.224	0.166	0.155	−0.159	0.252	0.166	0.171	8.3	10
Water	120000	120000	<0.02	0.217	0.137	0.155	−0.155	0.252	0.154	0.166	8.3	9.6
0.02% PAA	26000	22700	<0.02	0.295	0.058	0.102	−0.305	0.311	0.093	0.105	9.2	20
0.05% PAA	41000	32300	<0.03	0.305	0.059	0.111	−0.286	0.327	0.115	0.134	10.5	19
0.1% PAA	4000	600	<0.02	0.215	–	–	−0.223	0.230	–	–	–	32

data sets are included as a basis for comparison. The Newtonian fluid flows are also presented collectively and compared with data from the literature to establish confidence in the experimental apparatus and procedure, and to aid in the discussion of the non-Newtonian fluid flows.

For the water flows and the low-concentration PAA flows (0.02% and 0.05%) the velocity profiles exhibited axisymmetry (shown in Fig. 4(a)–(c)) and an apparent flowrate (determined from numerical integration of the velocity-profile data $\psi_R = 2\pi\int_0^R ur\,dr$) that deviated from the flowmeter by <5% in all cases and for the majority of profiles agreed to within 2%. Symmetry was always checked and confirmed (although with increased separation of the radial measurement locations beyond the centreline) at every measurement plane. Given the experimental uncertainty in measuring the velocities using LDA (Section 2) and the location of the wall together with the errors associated with the numerical technique to estimate the apparent flowrate, it appears reasonable to conclude that the mean flows are axisymmetric. For this reason, at all other locations only half profiles are reported for these flows. However, for the highest PAA concentration (0.1%), the mean axial velocity profiles did not display axisymmetry and so limited full profiles are reported for this fluid.

From the wall-pressure measurements shown in Fig. 5 it is evident that the effect of Reynolds number on the two water flows is minimal: the shape of the variation for the two flows is near-identical and the static-pressure recovery for both occurs well downstream of reattachment at about $x/h \approx 16$. The maximum recovery is only 2% below the Borda–Carnot value, $2\beta^2(1-\beta^2) = 0.375$ where β is the diameter ratio. For the two lowest concentrations of PAA (0.02 and 0.05%) the pressure variations are similar in shape to each other but with pressure recovery occurring much further downstream (at about $x/h = 25$) than for the water flows indicating a significant increase in the reattachment length compared to that for water. At the highest concentration of PAA (0.1%) the wall-pressure variation is significantly different to the water and low-concentration flows. Static-pressure recovery occurs even further downstream ($x/h \approx 40$) and is much lower in value at about 70% of the Borda–Carnot value. Due to the asymmetric nature (part D of this section) of this flow it would be misleading to draw any conclusions based on wall-pressure measurements obtained at a single circumferential location (see Fig. 1).

4.1.1. Newtonian fluid flow

Fig. 6a shows the mean axial velocity (U/U_B) profiles at various downstream locations for water flows with Reynolds numbers of $Re = 30{,}000$ and 120,000. Despite the four-fold difference in Re, the two flows reveal very similar mean axial velocity profiles. At the first measurement plane ($x/h = 1$) the higher Re flow has a thicker shear layer (represented by the vorticity thickness, δ_ω) and, associated with this, a slightly shorter reattachment length of 9.6 step heights compared to 10 step heights for the $Re = 30{,}000$ flow. The vorticity thickness δ_ω ($\equiv U_E/\dot{\gamma}_{MAX}$) at $x/h = 1$ is equal to 0.26 h for the high Re flow, approximately double the value for the lower Re flow. This Reynolds-number 'trend' is consistent with previously reported data, e.g. Escudier and Smith [12]. The growth rate of the vorticity thickness for both water flows is about the same, $d\delta_\omega/dx \approx 0.13$, as can be seen in Fig. 7. Escudier and Smith [12], using the same experimental set-up as in the present study but with an expansion of smaller area expansion ratio (2.37) observed a very similar value for the vorticity thickness growth. Both reattachment lengths are entirely consistent with values reported previously: Devenport and Sutton [4] list values in the range 8–11 step heights.

The maximum negative velocities within the recirculation region are almost identical (within 3%) at about $0.16U_B$, a value somewhat lower than was seen in the two-dimensional backward-facing step case ($0.22U_B$ as reported in [1,2] or Eaton and Johnston [24]) but identical to the value reported by Khezzar et al. [25] in their axisymmetric investigation.

The mean flow structure for the lower Reynolds number water flow is apparent from the streamline pattern shown in Fig. 8a which is based upon the stream function ψ evaluated numerically from the mean axial velocity distributions and defined as $\psi = 2\pi\int_0^r ur\,dr$ and plotted as ψ/ψ_R. The eye of the recirculation region is located approximately seven step heights upstream of reattachment (about $0.3x_R$) and just over half a step height from the wall in the y-direction. Table 3 shows that the maximum recirculating flowrate is about 8.3% of $\dot{Q}_A$ which is significantly higher than the equivalent value for the backward-facing step configuration (about 3.3% of $\dot{Q}_A$ [2]), presumably because a much larger volume of fluid must be entrained in the axisymmetric case before the flow reattaches.

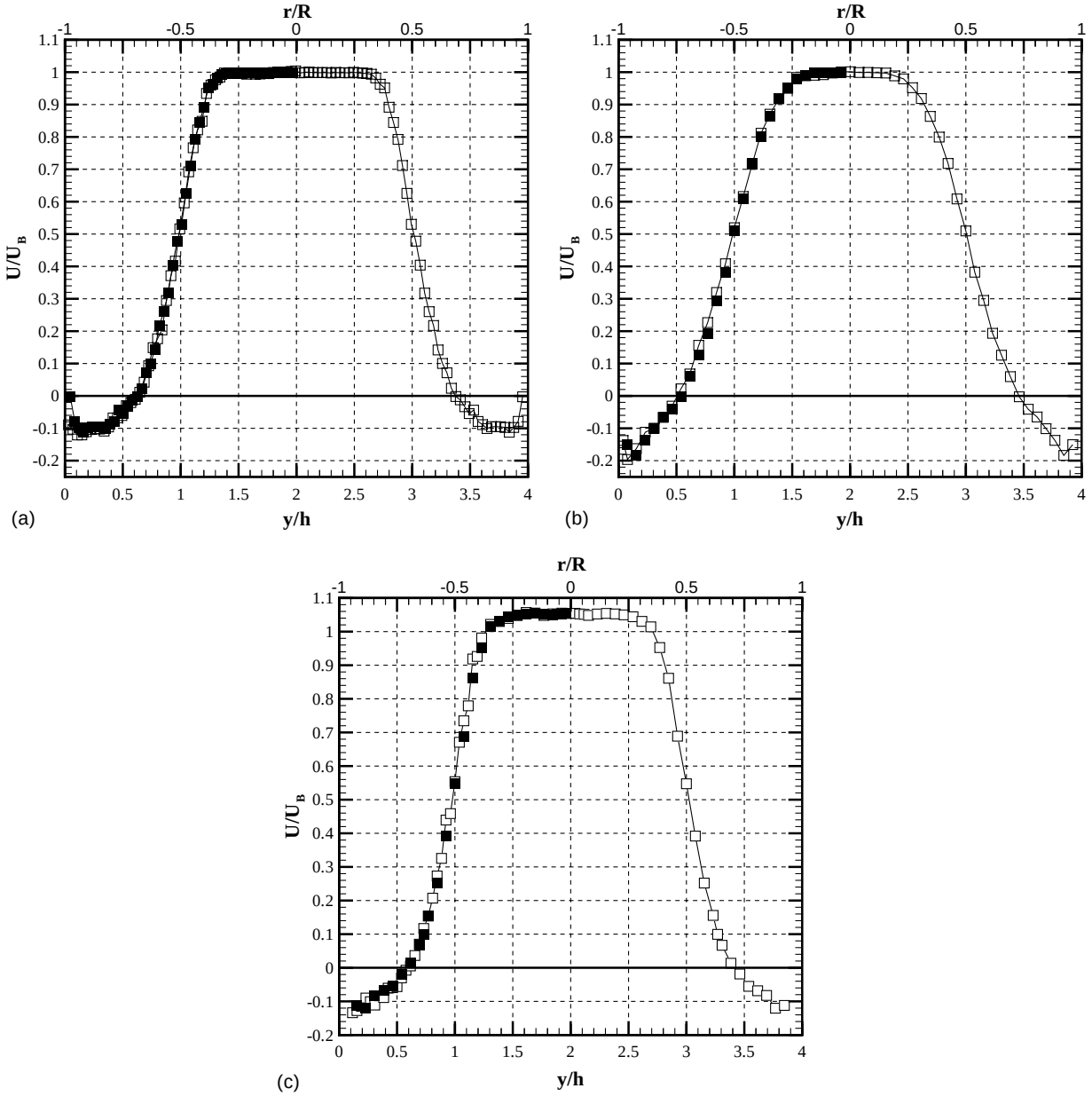

Fig. 4. (a–c) Symmetry of velocity profiles. (a) Water $Re = 30{,}000$ $x/h = 3$. (b) 0.02% PAA $Re = 26{,}000$ $x/h = 4$. (c) 0.05% PAA $Re = 30{,}000$ $x/h = 3$. [closed symbols are reflection about $r/R = 0$].

4.1.2. 0.02% PAA fluid flow, Re = 26,000

Included within Fig. 6b are the mean axial velocity profiles for 0.02% PAA at a Reynolds number of 26000 together with both water flows ($Re = 30{,}000$ and 120,000). The latter are included because one is at approximately the same Reynolds number ($Re = 30{,}000$), while the other has a very similar initial (i.e. at $x/h = 1$) shear-layer thickness. Although the profiles for 0.02% PAA are initially ($x/h < 4$) very similar to those for the water flows, major differences become apparent further downstream in the recirculation region. The reattachment length is approximately 20 step heights compared to about 9.6–10 h in the Newtonian case. This reattachment length is consistent with the value found by Pak et al. [14] (21 ± 4) h in their flow-visualisation study. (It was initially hoped to obtain 0.02% PAA results at a *Re* of approximately 50,000 but the fluid degradation time fell to the order of an hour or two (at best) so making detailed measurements with LDA a practical impossibility. We were able to measure the reattachment length however and we note that at a Reynolds of approximately 53,000 it was about 16 step heights.) Coupled with this increase in reattachment length is an increase in the magnitude of the recirculating velocities, especially in the range $5 < x/h < 12$: the maximum negative recirculating velocity is almost double the water value at $0.305U_B$.

The streamline pattern for this fluid flow, Fig. 8b, clearly shows a significant difference compared to the water flow with the streamline curvature in the shear layer being greatly

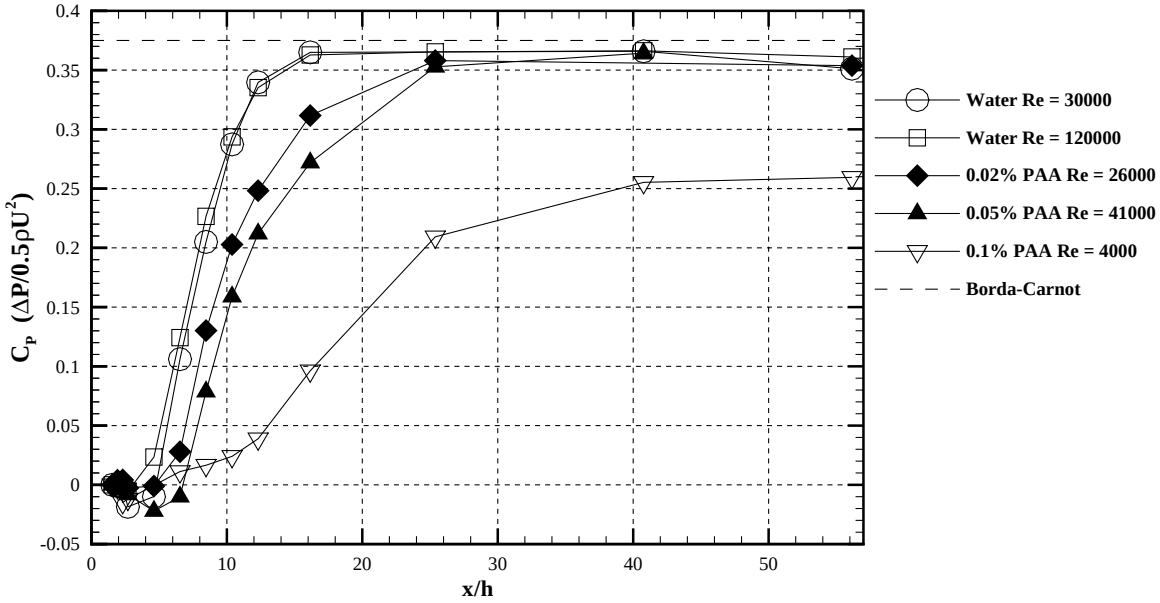

Fig. 5. Wall-pressure variation.

diminished for 0.02% PAA. The eye of the recirculation region is located approximately six step heights downstream of the step (about $0.3x_R$, which is similar to the value for water) and about 0.3 h from the wall in the *y*-direction. Table 3 shows that although the magnitudes of the recirculating velocities are significantly increased, the maximum recirculating flowrate (about 9.2% of $\dot{Q}_A$) is not much greater than for water. However, the axial variation of the vorticity thickness, Fig. 7, is significantly different from that for the water flows. At $x/h = 1$ the vorticity thickness δ_ω is comparable to that for water, by $x/h = 3$, it has increased slightly but is significantly below the corresponding water values. Between three and four step heights a large increase occurs in δ_ω before it becomes approximately constant in the range 4–10 h. This large increase may be due to the elastic molecules in the fluid being free to relax and so cause an expansion of the high-velocity core. Why this relaxation should occur some distance from the expansion and not immediately downstream of it is unclear although it could be related to the relatively high inertia of the high-velocity core.

At the final measuring location in Fig. 6b ($x/h = 20$) the viscoelastic fluid flow has only just reattached and the velocity distribution is significantly different in shape compared to the water profiles, which have become essentially uniform at this location.

4.1.3. 0.05% PAA fluid flow, Re = 41,000

Contained within Fig. 6c are the mean axial velocity profiles for 0.05% PAA at a Reynolds number of 41,000 together with both water flows ($Re = 30{,}000$ and 120,000). The first measurement profile (at $x/h = 1$) shows that the high-velocity core for this fluid is accelerated compared to both the water flows and the lowest concentration PAA flow with a velocity in the core of about $1.09U_B$. Presumably this acceleration is a consequence of the combination of the larger normal-stress difference produced by the flow through the smooth contraction that precedes the expansion. As we discuss in the following section, with increasing concentration the inlet velocity profiles produced by the smooth contraction become increasingly complex. The reattachment length for this fluid is 19 step heights, once again a large increase compared to the water flows but slightly less than for the lower concentration. Pak et al. [14] recorded a value of 25 ± 4 h for 0.05% PAA at a Reynolds number of approximately 5000. There are a number of possible reasons for the difference between our results and theirs. Their study had both a larger area expansion ratio (7.46) and a lower Reynolds number. An increased expansion ratio is known to result in an increase in the reattachment length for Newtonian fluids (Pereira and Pinho [7]) as is a decrease in Reynolds number, as found both here (part A) and by Escudier and Smith [12]. It must also be said that the flow-visualisation method used by Pak et al. [14] is rather crude, as is their use of the infinite-shear-rate viscosity in all their Reynolds number calculations which means that their *Re* values are considerably overestimated compared with our method of determining *Re*.

The axial variation of the vorticity thickness, Fig. 7, is similar in many respects to the lower concentration PAA flow with a large increase in δ_ω again evident between three and four step heights downstream of the expansion inlet. The similarity to the lower concentration flow is also apparent both from the streamline pattern, Fig. 8c, and also the increase in the magnitudes of the recirculating velocities listed in Table 3.

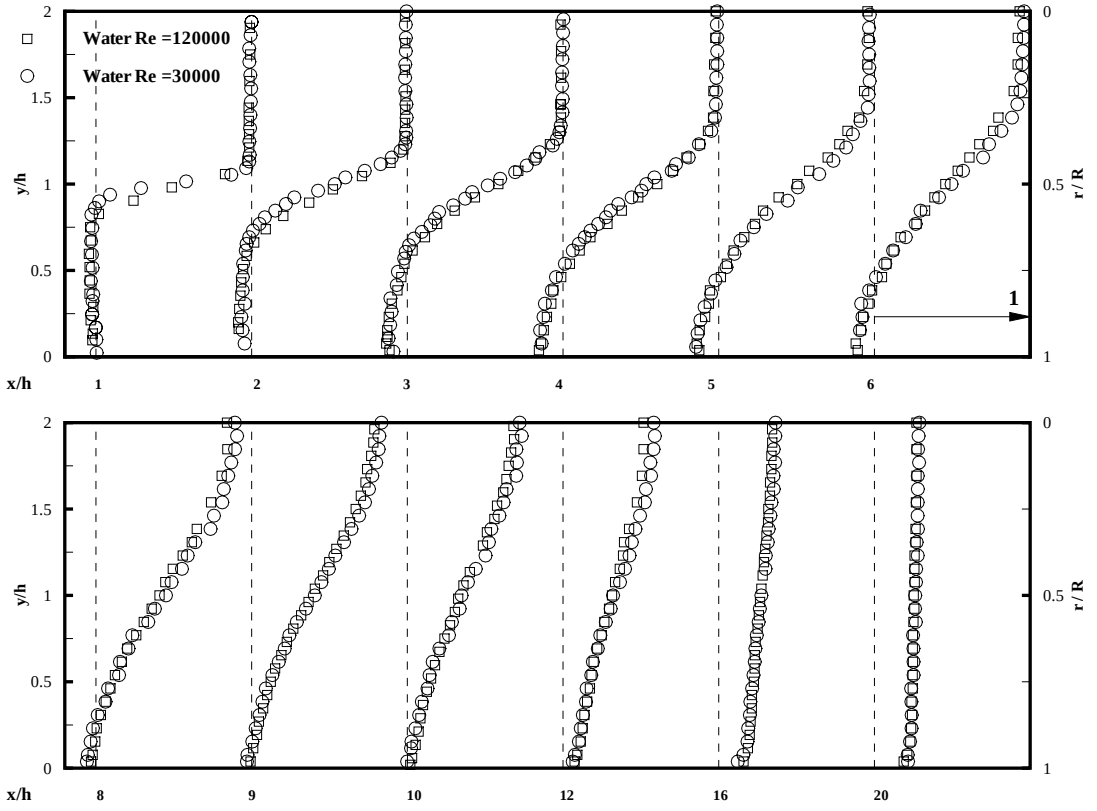

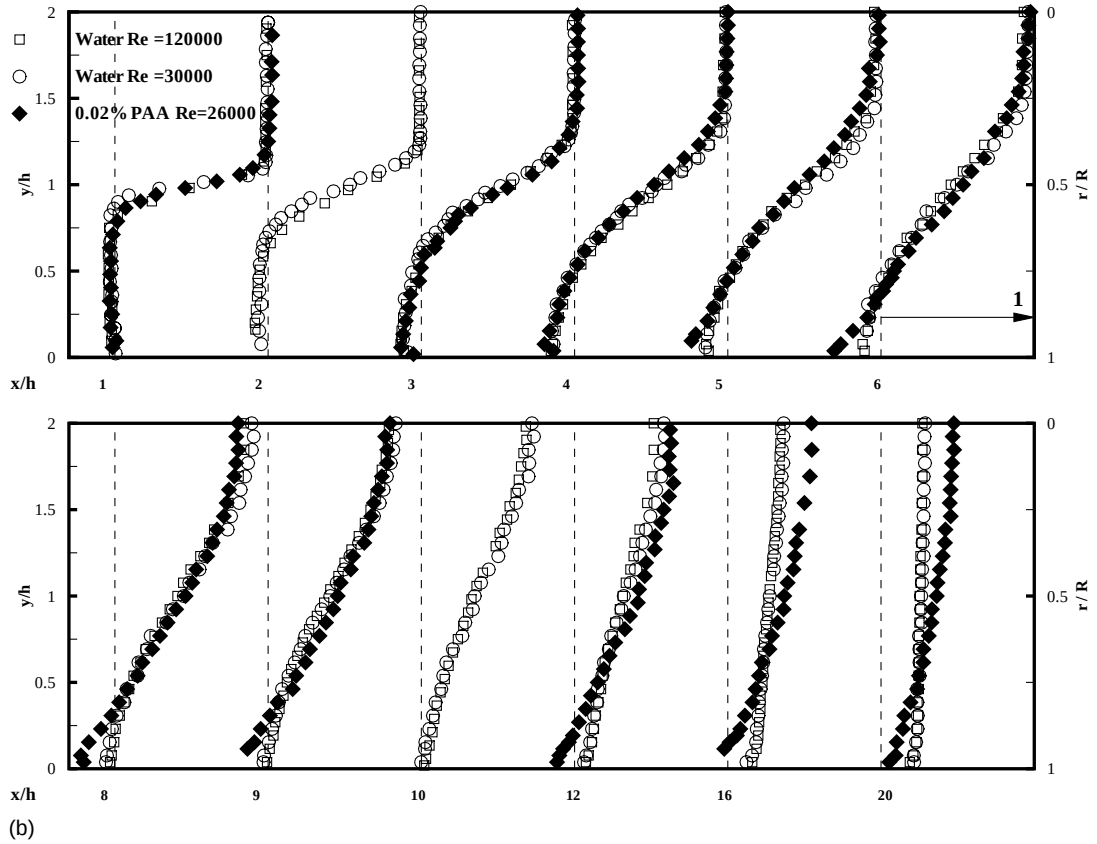

Fig. 6. (a–c) Mean axial velocity (U/U_B) profiles.

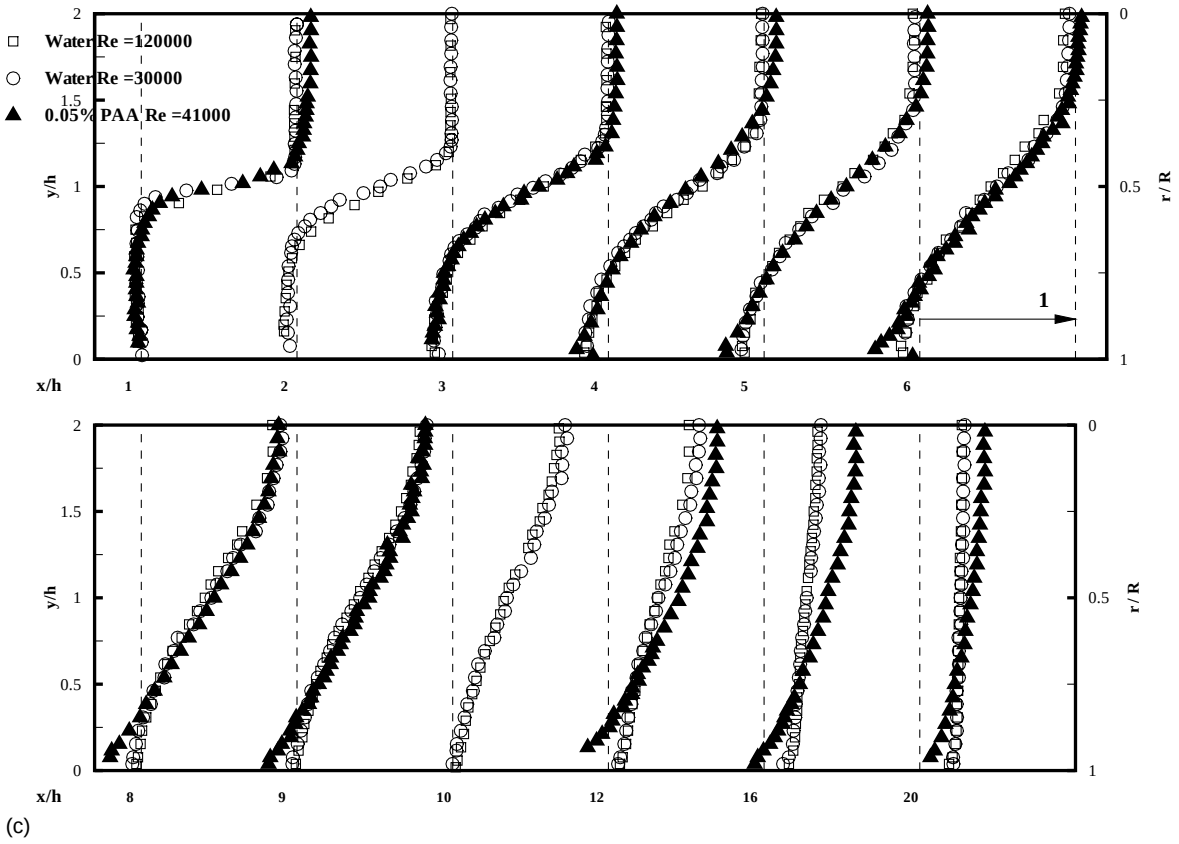

Fig. 6. (*Continued*).

4.1.4. 0.1% PAA fluid flow, Re = 4000

As already mentioned, the mean axial velocity profiles for 0.1% PAA did not exhibit axisymmetry despite symmetry existing for both the water and low-concentration PAA flows through this flow geometry. A number of measures were employed to determine the cause of the asymmetry. Initially (through an oversight) no flow straightener was included upstream of the pipe-flow run. The mean axial velocity profile in the absence of the flow straigtener measured one step height down from the expansion can be seen in

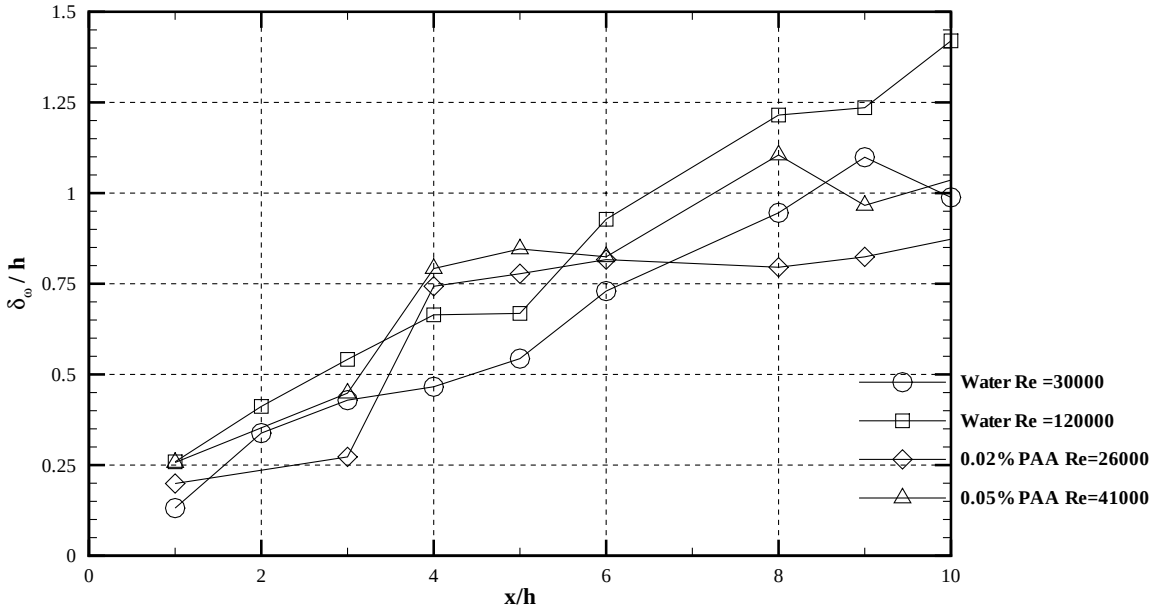

Fig. 7. Axial variation of the vorticity thickness.

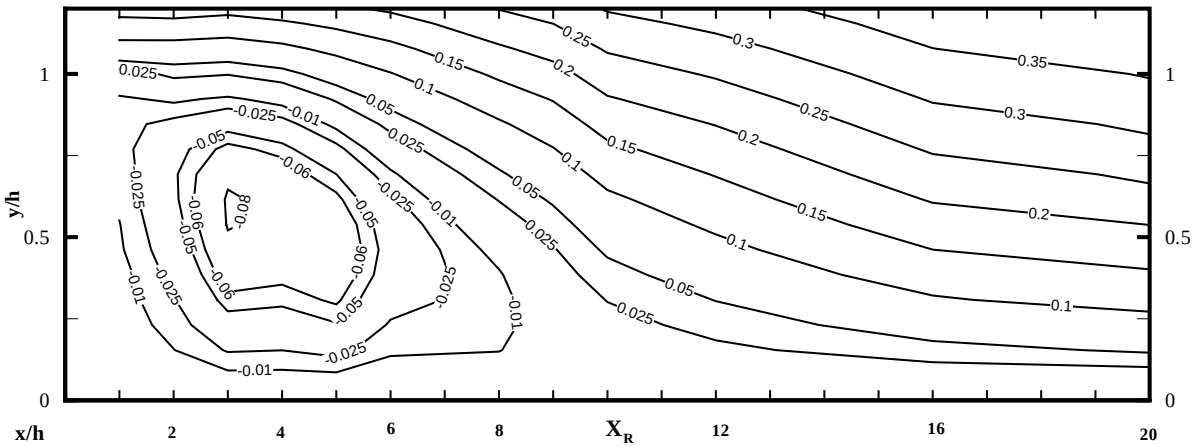

(a):Streamline pattern for Water Re=30000

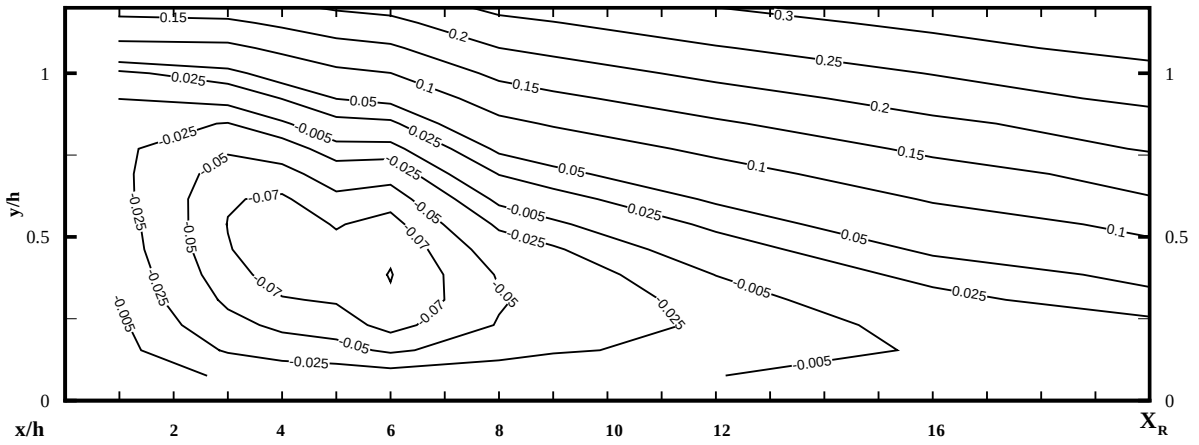

(b):Streamline pattern for 0.02% PAA Re=26000

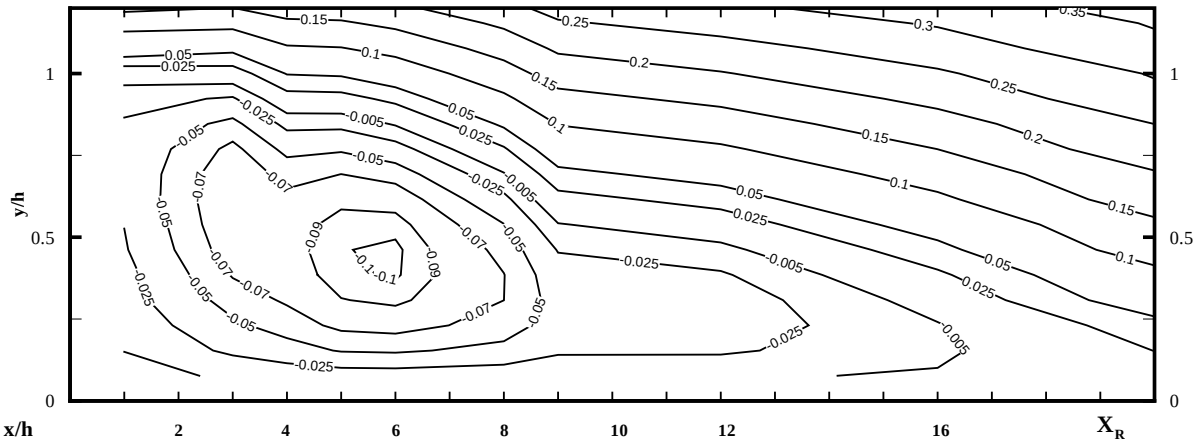

(c):Streamline pattern for 0.05% PAA Re=41000

Fig. 8. (a–c) Streamline patterns: values on contours $= \psi/\psi_R$.

Fig. 9a and is clearly asymmetric: the peak velocity is located away from the centreplane at $y/h = 1.5$. On the far side ($y/h > 2$) of the pipe the recirculating velocities are smaller than those for the near side ($y/h < 2$) and the width of the region of high turbulence intensity narrower (not shown in figure). Although the sudden expansion is preceded by over 12 m of straight pipe, it has been observed previously in our laboratory that for highly viscoelastic fluids a 'memory effect' of the inlet bend can exist and a substantial swirl component persist far downstream from the initial disturbance (Smith [26]). To minimise swirl, a honeycomb flow straightener was added 12 m upstream of the sudden expan-

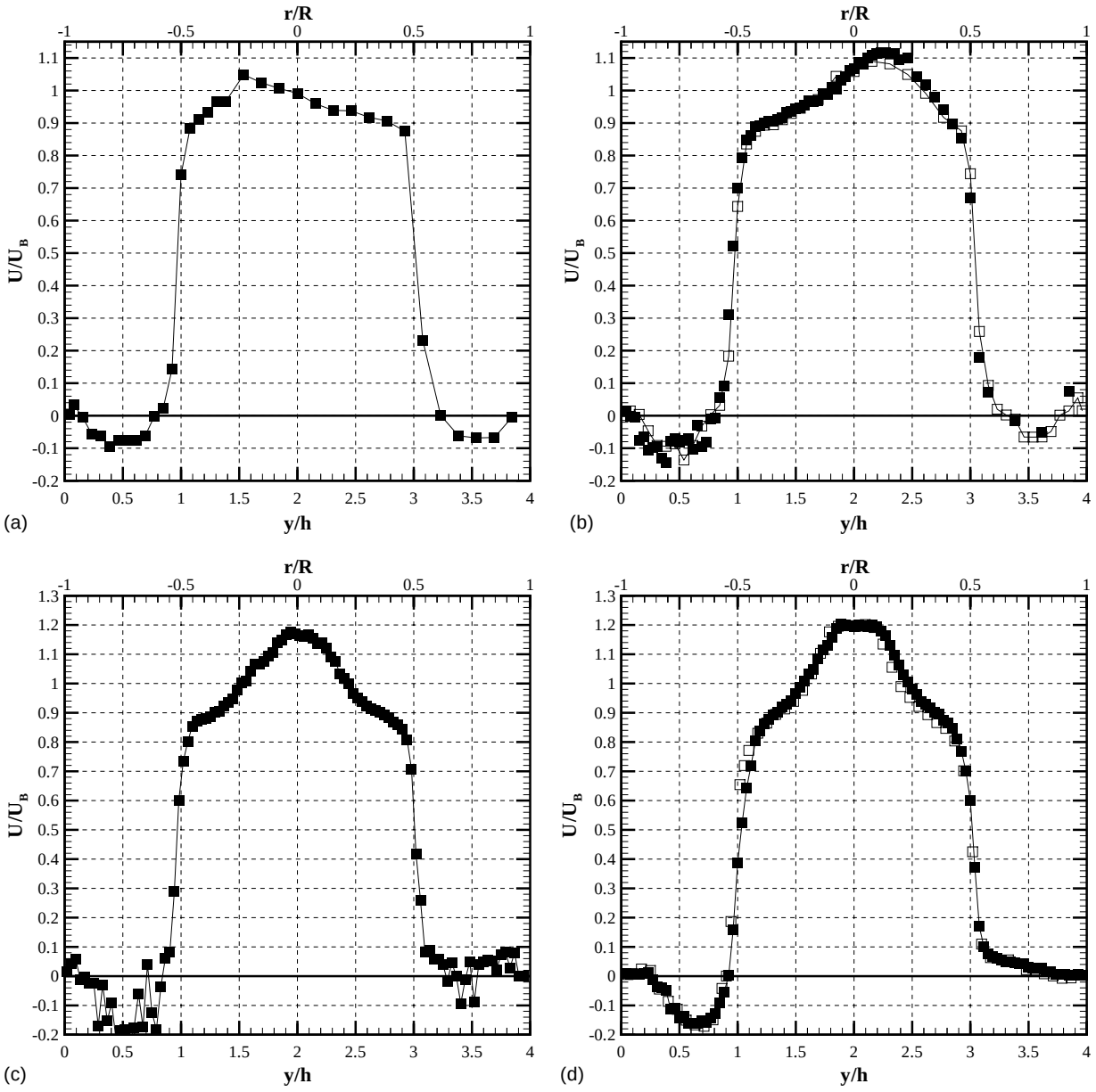

Fig. 9. (a–d) Mean axial velocity profiles at $x/h = 1$ for 0.1% PAA. (a) $Re = 34{,}000$ No flow straightener. (b) $Re = 34{,}000$ Honeycomb [closed symbols = repeat run]. (c) $Re = 12{,}000$ Honeycomb. (d) $Re = 4000$ Honeycomb [closed symbols] Flow straightener [open symbols].

sion (although this exacerbated the problem of fluid degradation). The results of the honeycomb on the axial velocity profile at $x/h = 1$ can be seen in Fig. 9b, a repeat run (with finer measurement point spacing depicted by the open symbols) was also conducted to confirm the results. Again the profile is clearly asymmetric, although in this instance the peak velocity occurs on the other side of the pipe. It was then decided to investigate the effects of Reynolds number: the results can be seen in Fig. 9c and d. Although the asymmetry in the high-velocity core diminishes as *Re* is decreased, in this measurement plane recirculating fluid is apparent on one side of the pipe but not the other. To further investigate the effect of the flow straightener the honeycomb was removed and replaced with a crossbeam arrangement (details are given in [27]), approximately 150 mm in length, which alleviated the problem of fluid degradation somewhat. The resulting profile at $x/h = 1$, also shown in Fig. 9d (open symbols), is almost identical to that with the honeycomb, despite these results being taken nine months apart and after the test section (i.e. sudden expansion) had been removed and reinstalled.

The foregoing can be summarised as follows. For Newtonian fluids and low concentration PAA flows the profiles are essentially symmetric and this suggests that geometric imperfections are not the cause of the asymmetry for 0.1% PAA. The addition of two different flow straighteners suggests that swirl is not the cause of the asymmetry although as *Re* is lowered the asymmetry in the high-velocity core

disappears to be replaced by another asymmetry on either side of the shear layer. It is suggested that the cause of the asymmetry is either: (a) an immeasurable geometric imperfection the effects of which are accentuated by high levels of viscoelasticity (i.e. large N_1) but attenuated for Newtonian and less elastic fluid flows; (b) an elastic instability arising due to a high Deborah number (De$\equiv\lambda/T_{CH}$ where T_{CH} is a characteristic time of the deformation process being observed (i.e. the flow) and λ is a characteristic time of the fluid) or (c) some other real effect of the fluid. Although Pak et al. [14] do not report asymmetric flow for 0.1% PAA, it is felt that their flow-visualisation technique is unlikely to have revealed such a characteristic. Due to the aforementioned difficulties, and the lack of symmetry, only a limited investigation (axial mean velocities and turbulence intensities) was conducted for this concentration of PAA.

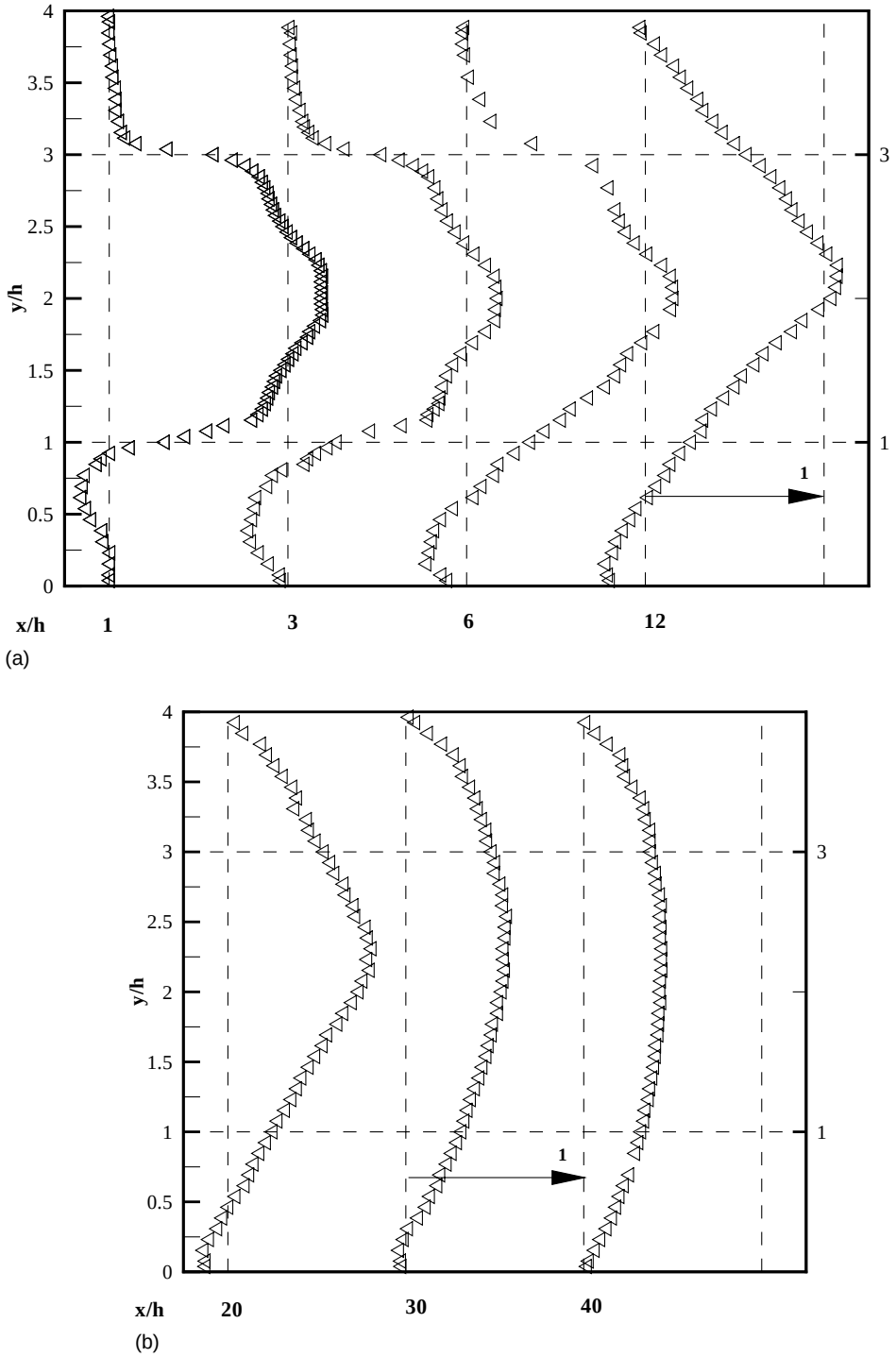

Fig. 10. (a–b) Mean axial velocity profiles for 0.1% PAA.

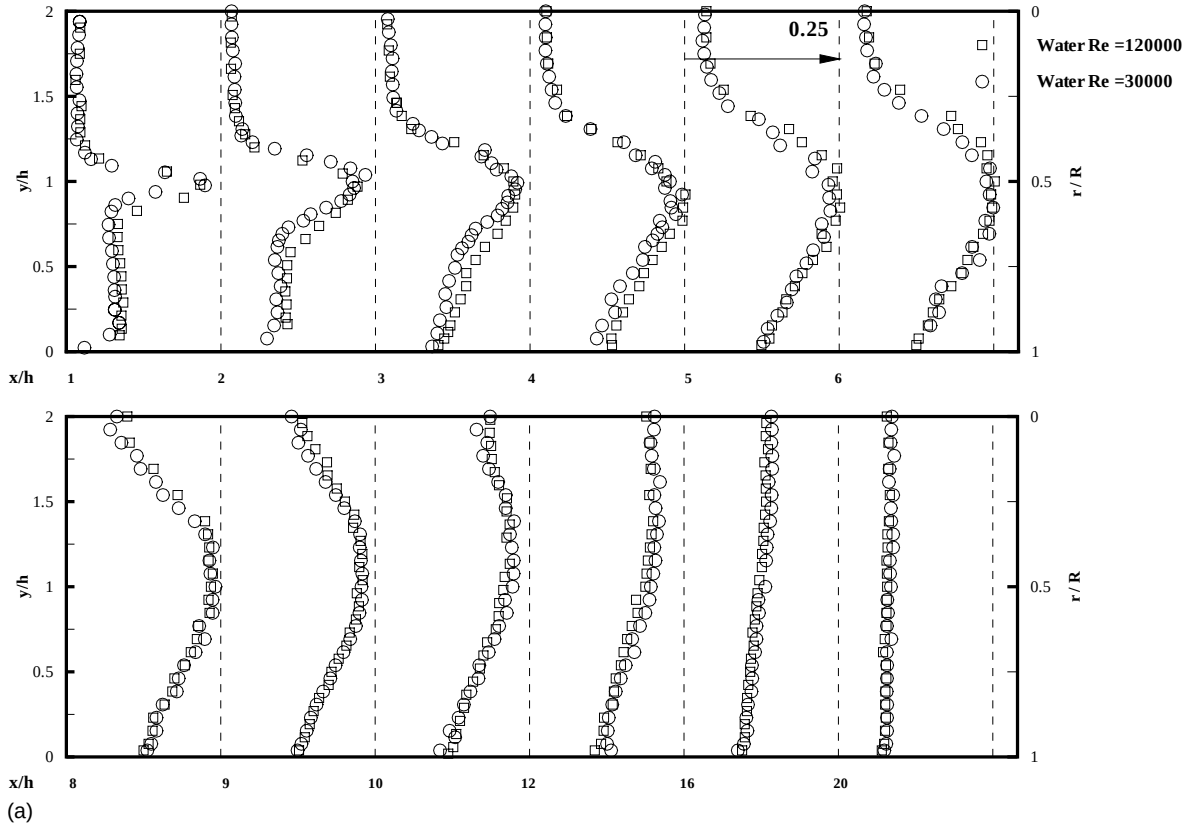

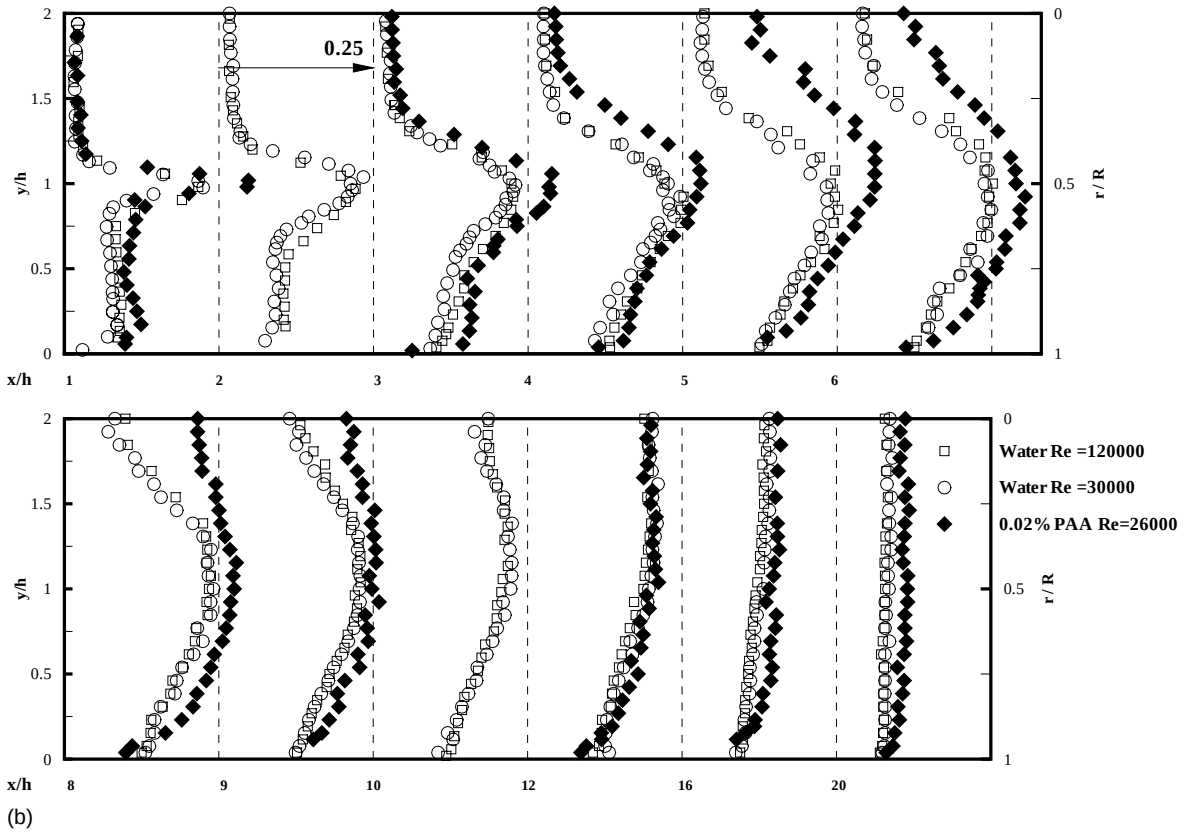

Fig. 11. (a–c) Axial turbulence intensity (u'/U_B) profiles.

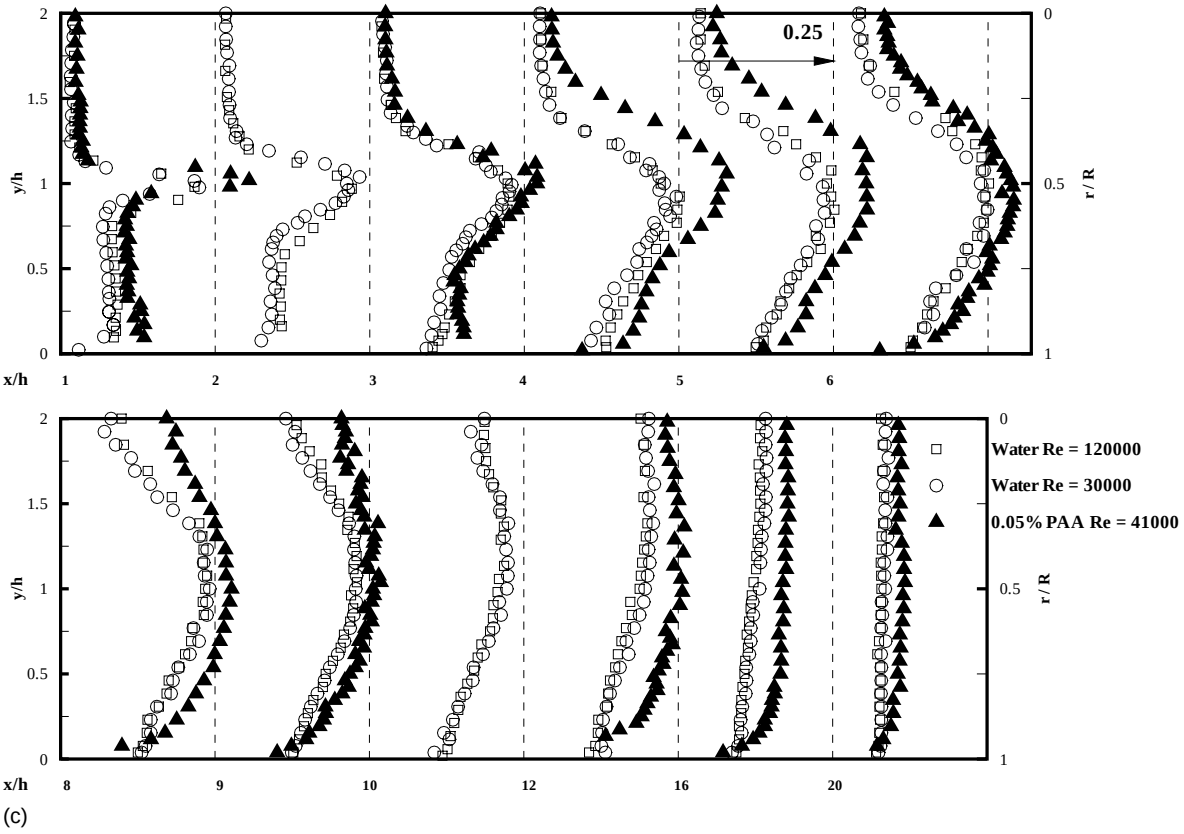

Fig. 11. (*Continued*).

The results of this limited investigation can be seen in Fig. 10a and b. As has been shown already, Fig. 9d, the inlet profile of the high-velocity core is far from uniform. The expected effect of a smooth contraction for a Newtonian fluid is well known: the generation of a uniform velocity profile. The experimental verification of this has effect been observed in the water flows in the current study (Fig. 6a). Quite clearly the inlet profile for 0.1% PAA is far from uniform: in the near vicinity of the pipe centreline ($1.75 < y/h < 2.25$) there is an accelerated central core of small diameter ($\sim d/4$) within which the velocity is uniform and about 20% greater than U_B. On either side of this core is an inflected velocity profile followed by a 'shoulder point' and then the shear layer resulting from the sudden expansion. The velocity profile is reminiscent of the laminar inlet velocity profile of a highly viscoelastic liquid (0.4% PAA) over the backward-facing step, as discussed in Poole and Escudier [28]. As the effect of shear thinning is normally to flatten the velocity profile it must be concluded that viscoelasticity is again the cause of the strongly non-uniform inlet profile observed here. So far as we are aware the effect of a smooth contraction on viscoelastic fluid flow at moderate to high Reynolds numbers has not been reported in the literature. The limited results obtained in our laboratory [1–3,28] reveal major differences compared with Newtonian fluid flows and suggest that a more extensive study is required.

As the flow progresses downstream the accelerated central core is smeared out but the asymmetry becomes more pronounced as the high-velocity core deflects towards the side that was initially not recirculating (i.e. $y/h = 4$). Negative velocities were not recorded near this pipe wall until $x/h = 6$ and the flow velocity had become positive again by $x/h = 20$ whereas on the opposite side recirculating fluid was evident until about 32 step heights downstream of the expansion. Even at $x/h = 40$ the flow is still asymmetric (Fig. 10b).

4.2. Turbulence structure

4.2.1. Newtonian fluid flow

Profiles of the r.m.s turbulence-intensity levels of all three velocity components (u', v' and w') are shown in Figs. 11a, 12a and 13a. As for the mean flow, the differences in the two water flows are slight and restricted to the wider initial shear layer of the higher *Re* flow resulting in initially broader regions of high turbulence intensity. The maximum turbulence levels (listed in Table 3) at the first measurement plane ($x/h = 1$) are in very close agreement which suggests that the slight difference in reattachment length is related to the initial width of the shear layer (i.e. initial vorticity thickness) rather than the maximum inlet turbulence intensity (in contrast to the backward-facing step data of [2]). The measured maximum values are virtually identical for

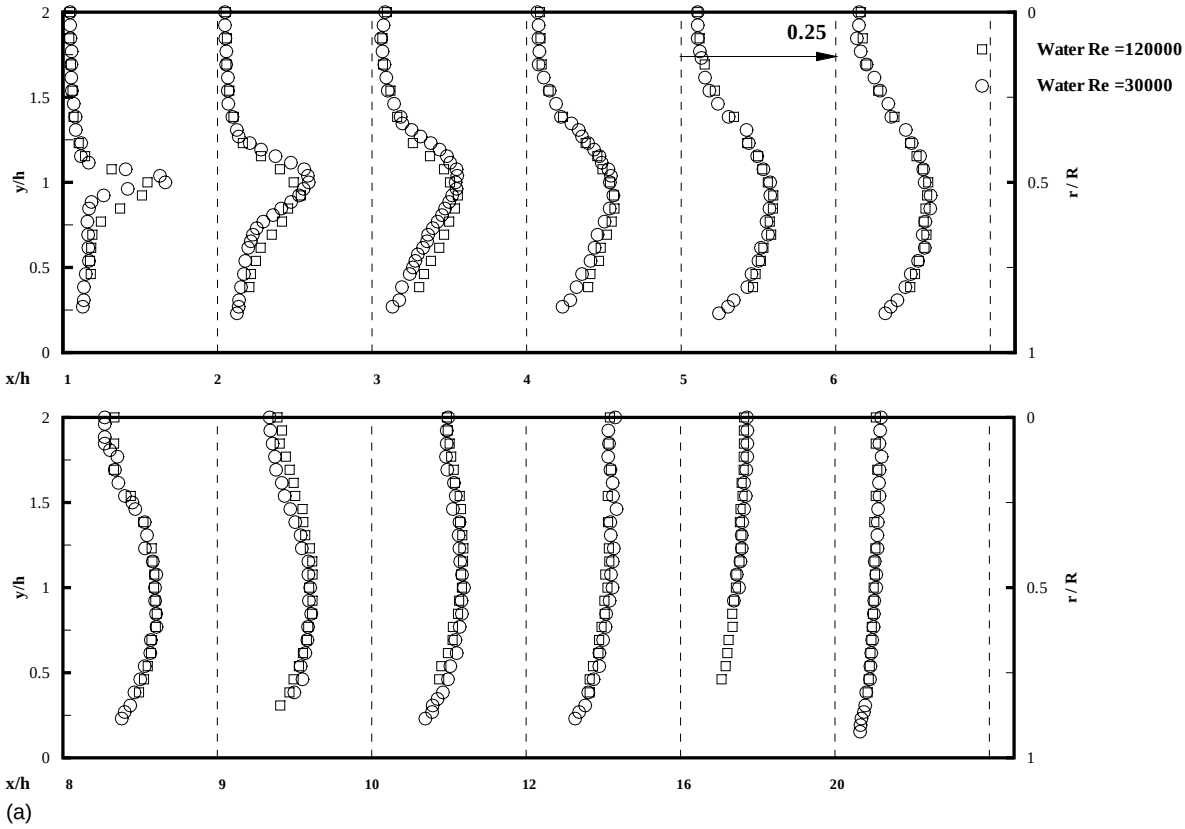

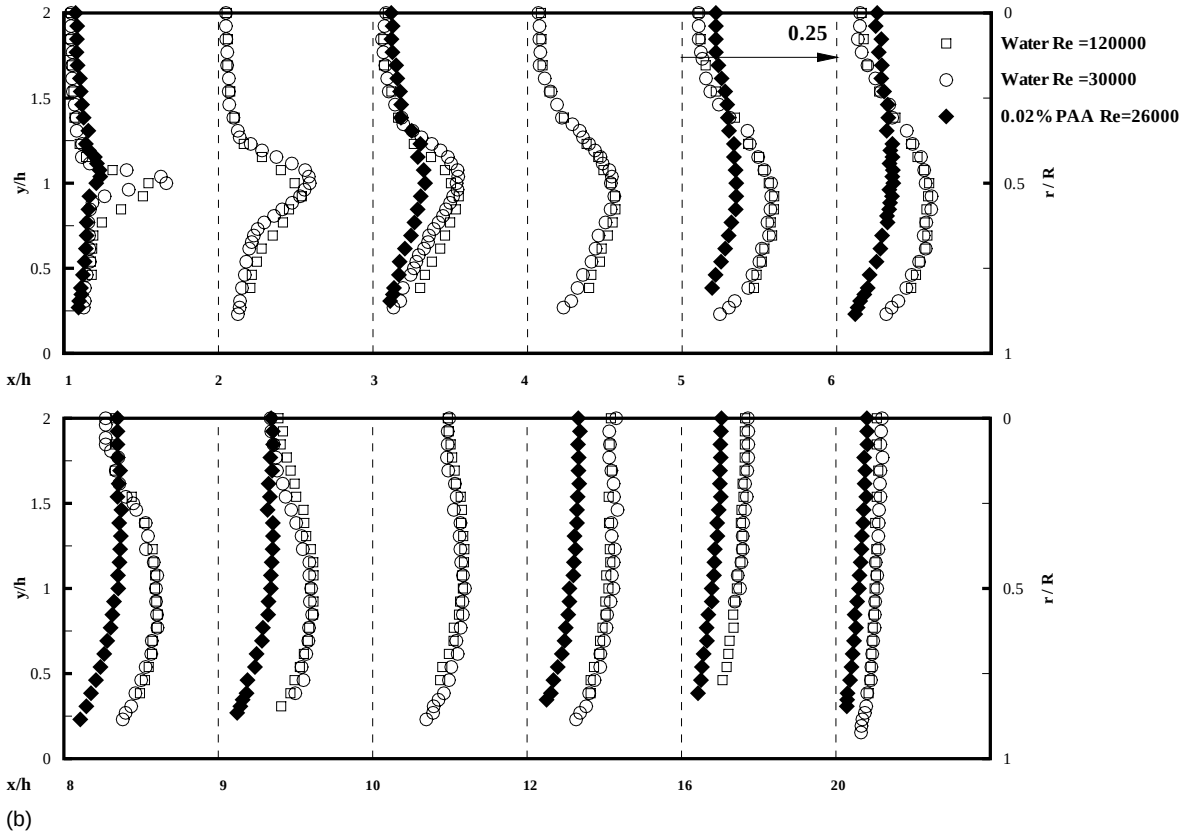

Fig. 12. (a–c) Radial turbulence intensity (v'/U_B) profiles.

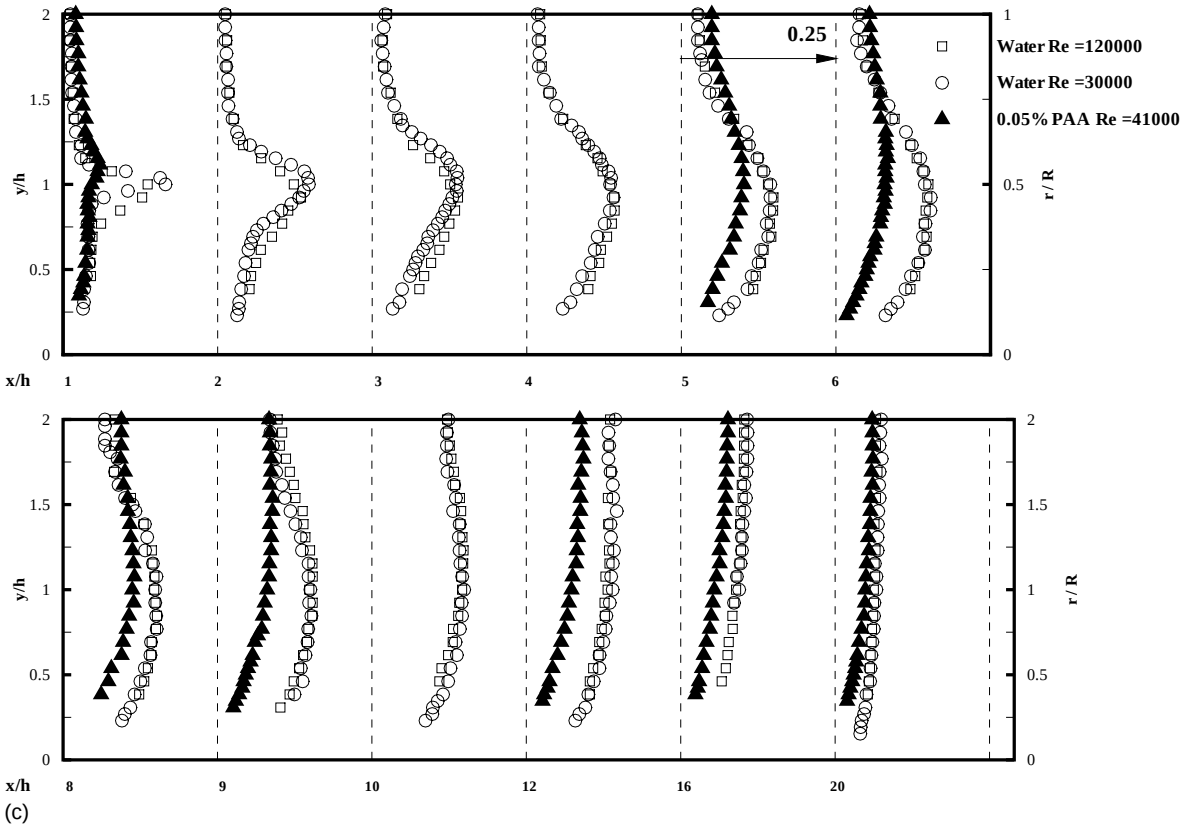

Fig. 12. (*Continued*).

the two flows: $u'_{MAX} = 0.25U_B$, $w'_{MAX} = 0.17U_B$ and $v'_{MAX} = 0.15U_B$. The ordering of the maximum intensities (i.e. $u' > w' > v'$) and corresponding degree of anisotropy are in agreement with all previous studies of axisymmetric sudden expansions. The magnitudes of the maxima are also consistent with published results for axisymmetric sudden expansions preceded by smooth contractions, as is the case here (e.g. Gould et al. [6] report $u'_{MAX} = 0.25U_B$ and $v'_{MAX} = 0.15U_B$). Axisymmetric sudden expansions with a fully-developed profile at inlet tend to have maximum turbulence intensities about 10–20% lower in magnitude [26]. At the final measuring location ($x/h = 20$), the profiles are essentially flat for all three components, although the turbulence is still anisotropic, u' being about 15% greater than both v' and w'.

4.2.2. 0.02% PAA fluid flow, Re = 26,000

Profiles of the r.m.s levels of all three turbulence components for 0.02% PAA are shown in Figs. 11b, 12b and 13b with the water-flow data included for comparison. As in our previous study of backward-facing step flow [1,2], the inlet turbulence levels have a significant effect on the mean flow for both Newtonian and non-Newtonian fluid flows. The maximum level for the axial turbulence intensity (Fig. 11b) at $x/h = 1$ is increased by about 35% (from about 0.22 to $0.31U_B$) compared to the water flow. This increase, if the tangential and radial turbulence intensities were unaltered, would be expected to have the effect of *decreasing* the reattachment length. However, the radial and tangential turbulence intensities at inlet (Figs. 12b and 13b, respectively) are greatly reduced compared to the water flow (maximum values of v' by over 50% from 0.14 to $0.06U_B$ and w' by over 30% from 0.16 to $0.1U_B$). This large reduction of v' both at inlet and elsewhere reduces the radial transfer of momentum and so must be a significant factor in increasing the reattachment length for this flow.

Fig. 11b shows that the axial turbulence intensity is everywhere higher compared to the water flows, reaching a maximum of $0.31U_B$, an increase compared to water of 23%. The regions of high axial turbulence intensity are also much wider for PAA compared to water (for example the profiles at $x/h = 5$ and 6) and even in the high-velocity core, where $\partial U/\partial y$ is small, high values of u' are still evident. The reduction seen at inlet ($x/h = 1$) for the radial and tangential turbulence intensities persists throughout the flowfield (Figs. 12b and 13b): downstream of $x/h = 3$ the profiles are essentially flat, with levels diminished in the shear layer compared to water and of about equal magnitude to each other. The maximum values for v' and w' are $0.09U_B$ and $0.11U_B$, respectively, reductions compared to water of about 40% in each case. Only in the high-velocity core between five and eight step heights downstream do the radial and tangential fluctuations exceed the Newtonian values, presumably a consequence of the greatly increased ax-

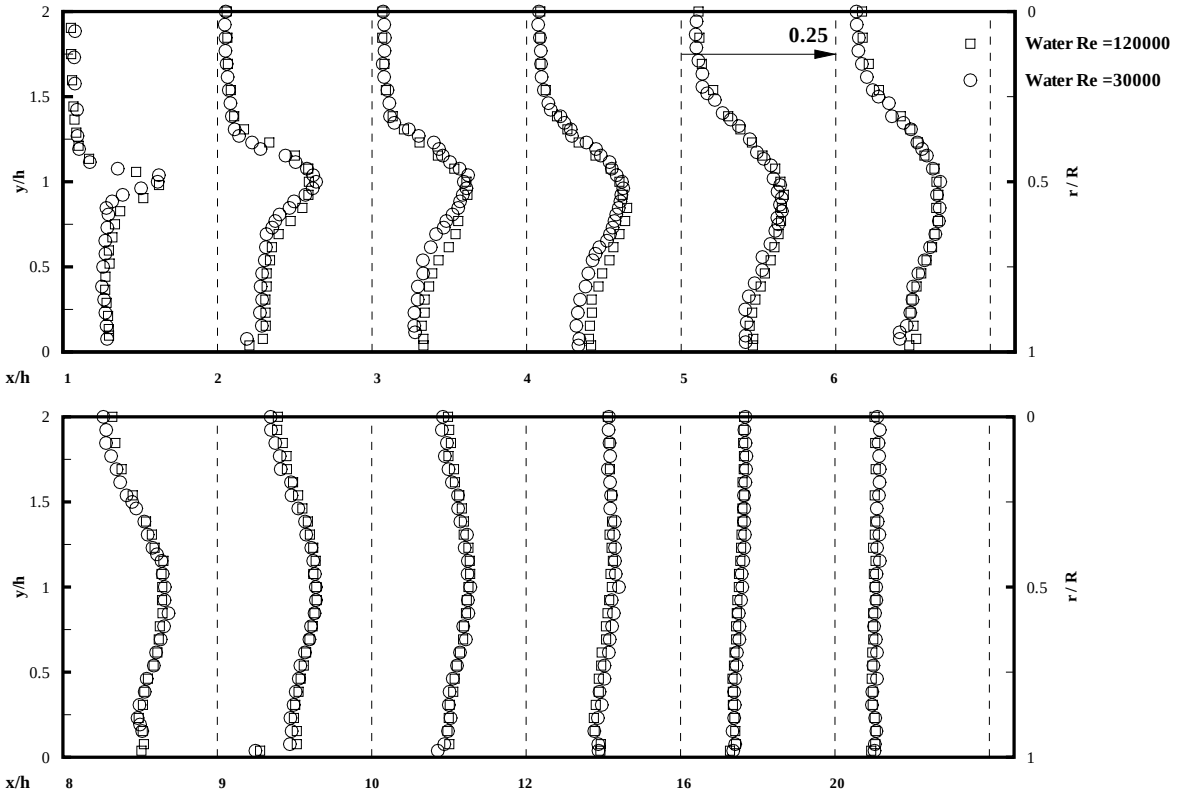

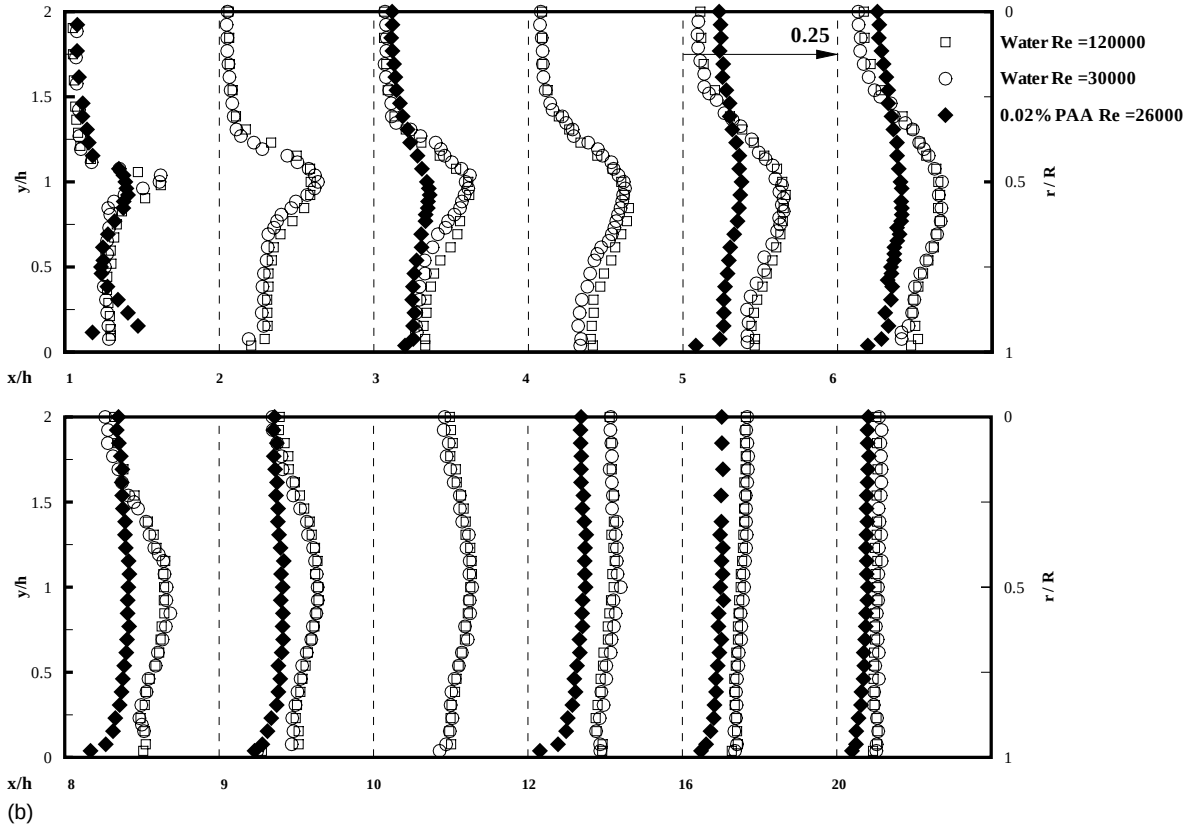

Fig. 13. (a–c) Tangential turbulence intensity (w'/U_B) profiles.

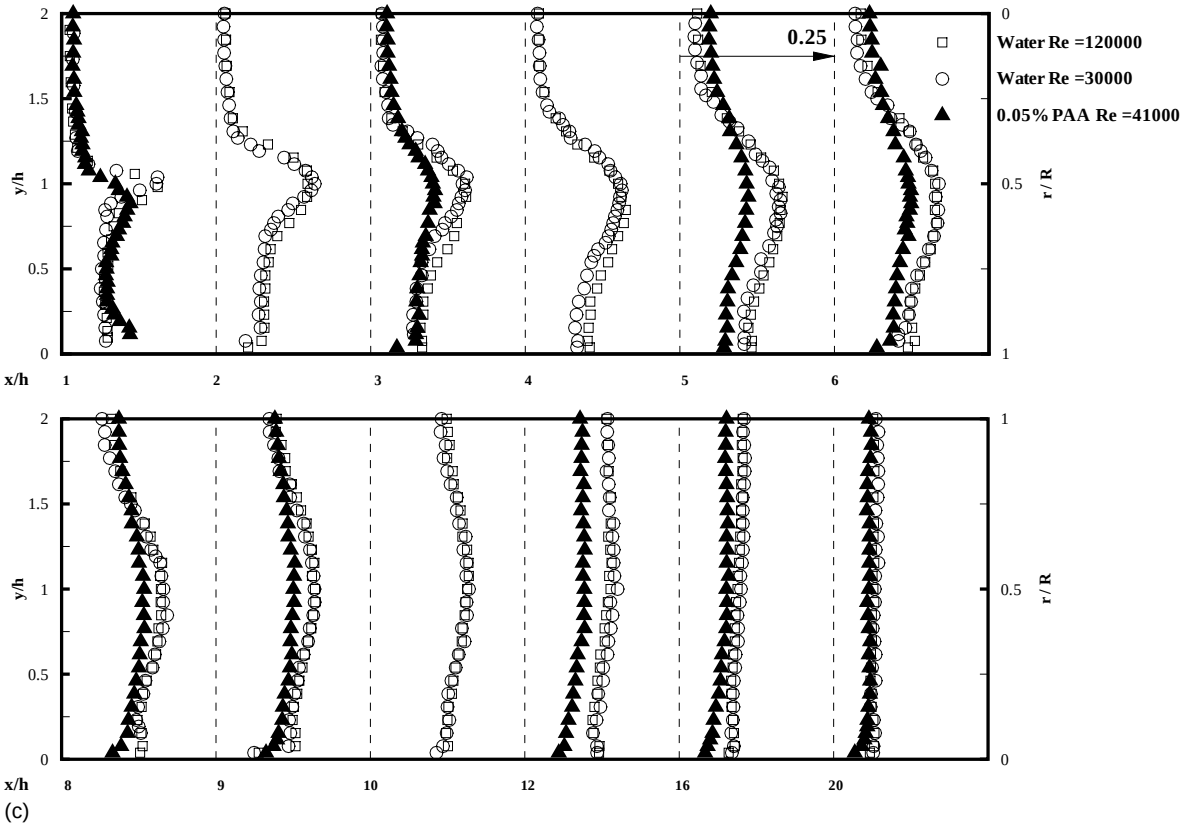

Fig. 13. (*Continued*).

ial turbulence intensity present in this region and the associated increases in v' and w', despite the large turbulence anisotropy.

Hibberd [29] also found that compared with the flow of water u' increased while both v' and w' decreased, for his two-dimensional shear-layer study with 50 ppm PAA. In contrast, Escudier and Smith [12] found that all three components were reduced compared to water for their experiments with 0.25% xanthan gum solution although these reductions were not sufficient to significantly affect the mean flow and the reattachment lengths were practically the same as for water. Castro and Pinho [9] used Tylose solutions (which are shear-thinning but of low elasticity) and again found reductions in all three turbulence components but only small variations in the recirculation length. From these results we conclude that it is primarily the molecular structure of non-Newtonian liquids which determines whether the reattachment length will be greatly altered compared to a Newtonian fluid. Although all three turbulence intensities are reduced for weakly elastic (so-called 'semi-rigid') polymers, such as xanthan gum, the corresponding degree of turbulence anisotropy is still quite similar to that for the Newtonian fluids. The corresponding turbulence transport mechanisms must be largely unaltered and so the reattachment length largely unaffected. In contrast the 'very flexible' PAA molecules lead to increased turbulence anisotropy with large reductions in v' (and w'), and the bulk of the turbulent kinetic energy being contributed by the axial component resulting in decreased radial transfer of momentum and large increases in the reattachment length.

4.2.3. 0.05% PAA fluid flow, $Re = 41{,}000$

The profiles of the r.m.s turbulence intensity levels of all three turbulence components (u', v' and w') for 0.05% PAA shown in Figs. 11c, 12c and 13c exhibit many features in common with the 0.02% PAA flow. Again at inlet the maximum axial turbulence intensity $\sim 0.3U_B$ is much greater than for the water flows and a high level of turbulence anisotropy exists: $v' < 0.2u'$ and $w' \approx 0.3u'$, values consistent with those for the 0.02% PAA flow.

The progression of the turbulence intensity profiles with downstream axial distance is again very similar to the lower concentration PAA flow. For 0.05% PAA the magnitudes of the maximum intensities are slightly higher (0.1–$0.2U_B$) than for 0.02% PAA and this accounts for the slightly shorter reattachment length for this flow, although the maximum v' and w' values are still much lower than those for water. The fact that there appears to be little effect of PAA concentration on both the mean flow and turbulence structure is probably related to the different Reynolds numbers of the two flows. As we discussed previously (Section 4.1.2) the

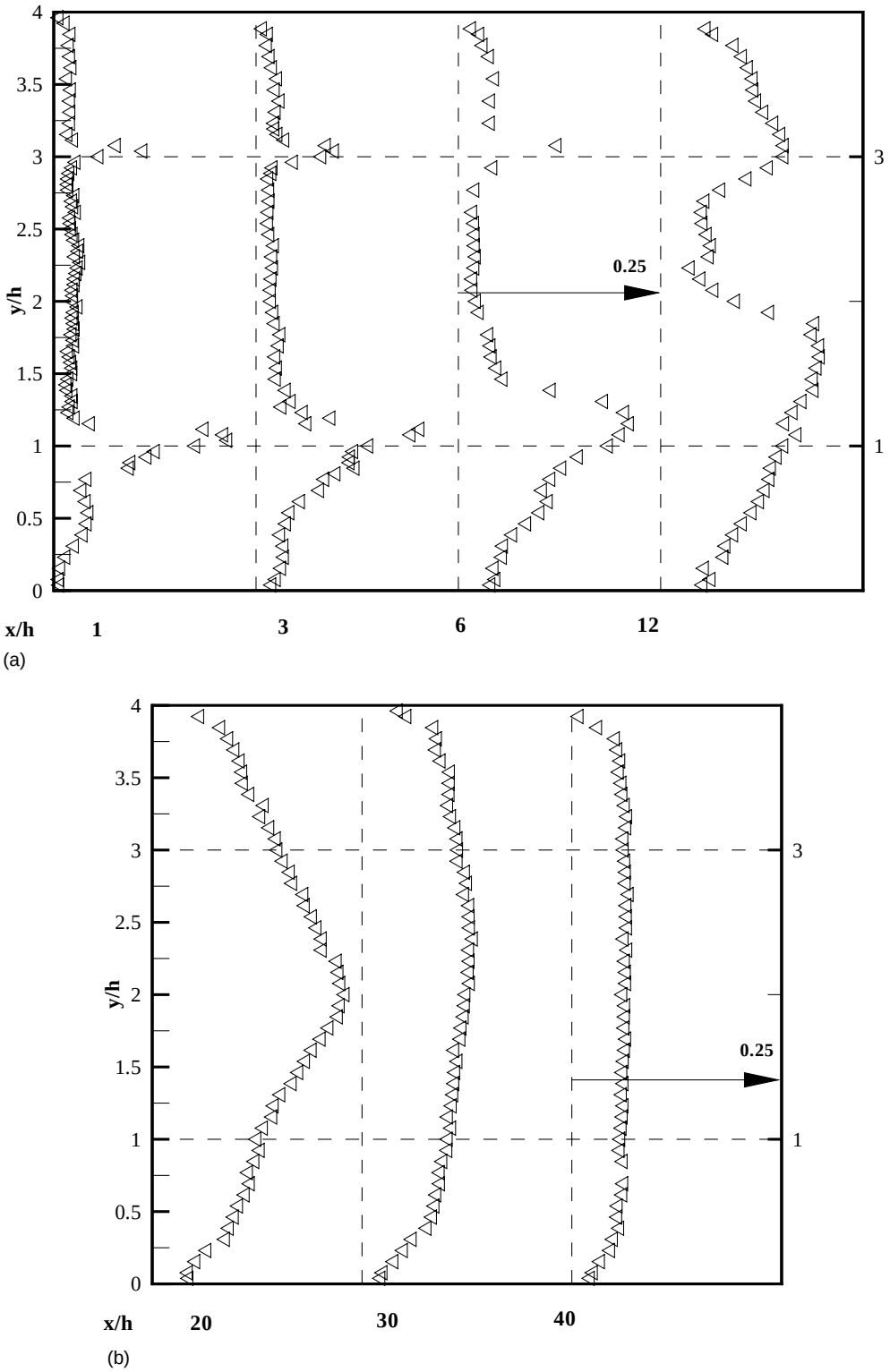

Fig. 14. (a–b) Axial turbulence intensity (u'/U_B) profiles for 0.1% PAA.

reattachment length for 0.02% PAA at $Re = 53{,}000$ was about 16 step heights and this suggests that increasing the concentration at a given *Re* would result in an increase in reattachment length consistent with the observations of Pak et al. [14].

4.2.4. 0.1% PAA fluid flow, $Re = 4000$

Limited profiles of axial turbulence intensity are shown for 0.1% PAA in Fig. 14a and b. The asymmetry of the flow is again apparent with larger intensities in the shear layer on the side $y/h < 2$, the side on which recirculating fluid was

seen at $x/h = 1$ in Fig. 10a. By $x/h = 20$ the two shear layers have merged and there is only one maximum located on the pipe centreline (i.e. $y/h = 2$). At the final measuring location, $x/h = 40$, the turbulence-intensity profile is almost symmetrical about the centreline despite the mean velocity profile still being asymmetric.

5. Conclusions

Results have been reported of an experimental investigation into the flow of three viscoelastic liquids (0.02, 0.05 and 0.1% PAA) and two water flows through an axisymmetric sudden expansion of area expansion ratio 4. For the water flows and the low concentration PAA flows (0.02 and 0.05%) the flows were axisymmetric. For the highest concentration of PAA, despite a number of changes to the flow loop, axisymmetric flow could not be achieved.

The reattachment lengths for the two water flows ($Re =$ 30,000 and 120,000) were 10 and 9.6 step heights, respectively, entirely consistent with values previously reported in the literature. The maximum turbulence intensities at inlet were almost identical and the slight difference in the reattachment length is probably attributable to the larger initial vorticity thickness of the higher *Re* flow.

For the lowest concentration of PAA at a Reynolds number of 26,000 the flowfield was significantly different than for the water flows. In agreement with the only previous study (Pak et al. [14]) the reattachment length was approximately doubled. In addition the magnitudes of the recirculating velocities were increased to almost double the corresponding water values. As the vorticity thickness was much the same as for the water flows the change in reattachment length must be related to the effects of viscoelasticity and in particular the radical restructuring of the turbulence. The axial turbulence intensity was amplified both at inlet and downstream of the expansion, compared to the water flows, with the maximum value almost 25% greater. A very high level of turbulence anisotropy was present both at inlet (where v' and w' were both $<0.3\ u'$) and further downstream (where v' and w' were again significantly reduced compared to the water values). This high level of anisotropy, with the bulk of the turbulent kinetic energy being contributed by the axial component and significantly reduced radial turbulence intensity, must play a significant role in decreasing the radial transfer of momentum and hence the increasing reattachment length.

The results for 0.05% PAA $Re = 41{,}000$ were consistent with the lower concentration results. The slightly shorter reattachment length for this flow (19 h) is attributable to the increased Reynolds number. This conclusion was confirmed by measuring the reattachment length for 0.02% PAA at a Reynolds number of about 50,000 where it was found that the reattachment length was reduced from 20 h (for $Re =$ 26,000) to approximately 16 step heights.

For the highest concentration, 0.1% PAA, axisymmetric flow could not be achieved. It is suggested that the cause of the asymmetry is either (a) an immeasurable geometric imperfection the effect of which is accentuated by high levels of viscoelasticity (i.e. large N_1) but attenuated for viscous flows, (b) an elastic instability arising due to the high Deborah number or (c) some other real effect of the fluid. Further experiments are needed to clarify the exact cause.If we compare the results from the present study with our other recent work on the turbulent flow of viscoelastic and shear-thinning liquids over a backward-facing step [2] and through a plane sudden expansion [3], it is possible to draw some general conclusions about such flows. As Escudier and Smith (1999), Castro and Pinho (1995) and Pereira and Pinho (2000) have previously observed, the effect of shear thinning appears to be minimal. However, for low concentrations of PAA, the effects are extreme. Although such fluids are only very slightly shear-thinning and produce normal-stress differences which are too low to measure, they are still strongly drag-reducing, which is probably related to the extensional viscosity [17,18]. For these fluids, large increases in the reattachment length have been observed, ranging from 25% in the backward-facing step case [2] to 200% in the axisymmetric case. The smaller increase for the backward-facing step is related to the much smaller area expansion ratio for this geometry compared to the axisymmetric situation. Large increases are also observed in the recirculating velocities and recirculating flowrates. Much as is the case for drag reduction, we suggest the increase in the reattachment length is related to the way in which the polymer molecules alter the turbulence structure. The axial (streamwise) component is accentuated compared to water, while v' and w' are attenuated. The combination of these effects is an enhanced level of turbulence anisotropy (compared to water) which leads to reduced transport of radial (transverse) momentum and hence increased reattachment lengths.

At higher PAA concentrations three-dimensional effects become more pronounced, the likely cause of which is larger normal-stress differences. These three-dimensional effects are most easily seen in the plane sudden-expansion geometry [3] but are also present for the backward-facing step flow in laminar flow [28] and downstream of reattachment in turbulent flow. The lack of mean flow axisymmetry in the current study for 0.1% PAA could also be related to larger values of N_1. Large increases in the reattachment length again occur although the magnitudes of the recirculating velocities and flowrate are strongly reduced.

Despite the insights revealed by the studies to date, much further work needs to be conducted before a full understanding of turbulent sudden-expansion flow for non-Newtonian liquids is achieved.

References

[1] R.J. Poole, M.P. Escudier, Turbulent flow of non-Newtonian liquids over a backward-facing step. Part I. A thixotropic and shear-thinning liquid, J. Non-Newtonian Fluid Mech. 109 (2003) 177.

[2] R.J. Poole, M.P. Escudier, Turbulent flow of non-Newtonian liquids over a backward-facing step. Part II. Viscoelastic and shear-thinning liquids, J. Non-Newtonian Fluid Mech. 109 (2003) 193.
[3] R.J. Poole, M.P. Escudier, Turbulent flow of a viscoelastic shear-thinning liquid through a plane sudden expansion of modest aspect ratio, J. Non-Newtonian Fluid Mech. 112 (2003) 1.
[4] W.J. Devenport, E.P. Sutton, An experimental study of two flows through an axisymmetric sudden expansion, Exp. Fluids 14 (1993) 423.
[5] R.M.C. So, Inlet centreline turbulence effects on reattachment length in axisymmetric sudden-expansion flows, Exp. Fluids 5 (1987) 424.
[6] R.D. Gould, W.H. Stevenson, H.D. Thompson, Investigation of turbulent transport in an axisymmetric sudden expansion, AIAA J. 28 (2) (1989) 276–283.
[7] A.S. Pereira, F.T. Pinho, The effect of the expansion ratio on a turbulent non-Newtonian recirculating flow, Exp. Fluids 32 (2002) 458–471.
[8] N. Kasagi, A. Matsunaga, Three-dimensional particle-tracking velocimetry measurement of turbulence statistics and energy budget in a backward-facing step flow, Int. J. Heat Fluid Flow 16 (1995) 477–485.
[9] O.S. Castro, F.T. Pinho, Turbulent expansion flow of low molecular weight shear-thinning solutions, Exp. Fluids 20 (1995) 42–55.
[10] A.S. Pereira, F.T. Pinho, Turbulent characteristics of shear-thinning fluids in recirculating flows, Exp. Fluids 28 (2000) 266–278.
[11] A.S. Pereira, F.T. Pinho, Recirculating turbulent flows of thixotropic fluids, J. Non-Newtonian Fluid Mech. 99 (2001) 183–200.
[12] M.P. Escudier, S. Smith, Turbulent flow of Newtonian and shear-thinning liquids through a sudden axisymmetric expansion, Exp. Fluids 27 (1999) 427–434.
[13] K. Isomoto, S. Honami, The effect of inlet turbulence intensity on the reattachment process over a backward-facing step, J. Fluids Eng. 111 (1989) 87–92.
[14] B. Pak, Y.I. Cho, S.U. Choi, Separation and reattachment of non-Newtonian fluid flows in a sudden expansion pipe, J. Non-Newtonian Fluid Mech. 37 (1990) 175–199.
[15] C. Tropea, Laser Doppler anemometry: recent developments and future challenges, Meas. Sci. Technol. 6 (1995) 605–619.
[16] W.J. Yanta, R.A. Smith, in: Proceedings of the 11th Aerospace Science Meeting of the Measurements of Turbulence-Transport Properties with a Laser-Doppler Velocimeter, AIAA paper 73, Washington, 1973, pp. 169–179.
[17] M.P. Escudier, F. Presti, S. Smith, Drag reduction in the turbulent pipe flow of polymers, J. Non-Newt. Fluid Mech. 81 (1999) 197–213.
[18] J.M.J. den Toonder, M.A. Hulsen, G.D.C. Kuiken, F.T.M. Nieuwstadt, Drag reduction by polymer additives in a turbulent pipe flow: numerical and laboratory experiments, J. Fluid Mech. 337 (1997) 193–231.
[19] J.R. Stokes, L.J.W. Graham, N.J. Lawson, D.V. Boger, Swirling flow of viscoelastic fluids. Part 1. Interaction between inertia and elasticity, J. Fluid Mech. 429 (2001) 67–115.
[20] K. Walters, A.Q. Bhatti, N. Mori, in: D. De Kee, P.N. Kaloni (Eds.), The influence of polymer conformation on the rheological properties of aqueous polymer solutions, Recent Developments in Structured Continua, vol. 2, Pitman, 1990.
[21] K. Yasuda, R.C. Armstrong, R.E. Cohen, Shear flow properties of concentrated solutions of linear and star branched polystyrenes, Rheo Acta 20 (1981) 163–178.
[22] M.P. Escudier, I.W. Gouldson, A.S. Pereira, F.T. Pinho, R.J. Poole, On the reproducibility of the rheology of shear-thinning liquids, J. Non-Newt. Fluid Mech. 97 (2001) 99–124.
[23] H.A. Barnes, J.F. Hutton, K. Walters, An Introduction to Rheology, Elsevier, 1989.
[24] J.K. Eaton, J.P. Johnston, A review of research on subsonic turbulent flow reattachment, AIAA J. 19 (1981) 1093–1100.
[25] L. Khezzar, J.H. Whitelaw, M. Yianneskis, Round sudden-expansion flows, Proc. Instn. Mech. Eng. 200 (C6) (1986) 447–455.
[26] S.E. Smith, Turbulent Duct Flow of Non-Newtonian Liquids, Ph.D. Thesis, Department of Engineering, The University of Liverpool, 2000.
[27] R.J. Poole, Turbulent Flow of Newtonian and Non-Newtonian Liquids Through Sudden Expansions, Ph.D. Thesis, Department of Engineering, The University of Liverpool, 2002.
[28] R.J. Poole, M.P. Escudier, Laminar viscoelastic flow through a plane sudden expansion, in: Proceedings of the Eleventh International Symposium on Applications of Laser Techniques to Fluid Mechanics, Lisbon, Portugal, 8–11 July 2002, Paper 31-4.
[29] M.F. Hibberd, Influence of polymer additives on turbulence in a mixing layer, in: B. Gampert (Ed.), Proceedings of the Symposium of The Influence of Polymer Additives on Velocity and Temperature Fields, Berlin, Springer, 1985.